AN INTRODUCTION TO ROTATIONAL DEGREES OF FREEDOM OF SOLID MOLECULES

Dr. Mahesh Chandra Mishra

Kripa Drishti Publications, Pune.

AN INTRODUCTION TO

ROTATIONAL DEGREES OF FREEDOM OF

SOLID MOLECULES

Dr. Mahesh Chandra Mishra

Kripa-Drishti Publications, Pune.

Book Title: **An Introduction to Rotational Degrees of Freedom of Solid Molecules**

Author by: **Dr. Mahesh Chandra Mishra**

1st Edition

ISBN: **978-81-949998-9-8**

Published: **November 2019**

Publisher:

Kripa-Drishti Publications

A-503 Poorva Heights, Pashan-Sus Road, Near Sai Chowk,

Pune – 411021, Maharashtra, India.

Mob: +91-8007068686

Email: editor@kdpublications.in

Web: https://www.kdpublications.in

PREFACE

Recently many interests have been shown to study the rotational motion of molecules in solids of alkali halide crystals doped with polar impurities which shows pronounced effects on optical, thermal and electrical properties of the host crystals, playing a dominant role in science and technology.

A free molecule containing N atoms has 3N-6 degree of vibrational freedom, three degree of translational freedom and three degrees of rotational freedom. When a molecule is introduced substitutionally into a lattice, the vibrational degrees of freedom are usually changed relatively small by the matrix. The translational degrees of freedom of the molecules are the same as the translational degrees of freedom of an impurity atom, i.e., they manifest themselves as impurity modes. We have considered the third group of degree of freedom, those connected with the rotational inertia of the molecule.

Low temperature infra-red absorption, thermal conductivity and specific heat measurements have shown a better agreement with the theoretical one by optical spectroscopy method on Devonshire model. This model explains gross features of the IR data except the tunneling translations which were not observed in optical measurements that have been discussed in details.

By means of infrared-absorption, thermal-conductivity, and specific-heat measurements at low temperatures, the problem of rotational motion of molecules in solids has been studied using CN^- ions substituted for the halogen in KCl, KBr, KI, RbCl, NaCl, and NaBr. Energy levels associated with the ion performing free rotation, hindered rotation, oscillation, and tunneling motion were observed. It was found that a simple 3-dimensional potential for a linear diatomic molecule developed by Devonshire based on a 2-dimensional cosine potential first proposed by Pauling explained all of our observations.

For the potassium halides the barrier height is 0.003 eV; in RbCl it is 0.0075 eV, and in the sodium halides it is >0.015 eV. Stress experiments show that the ion has 6 equilibrium orientations along the 〈100〉 directions. Strong phonon scattering by tunneling states and rotational states is observed.

INDEX

ISBN: 978-81-949998-9-8

Chapter 1

Introduction

1.1 Introduction:

Infra-red absorption, thermal conductivity and specific heat measurements at low temperatures are the best tools for the problem of rotational motion of molecules in solids has been studied using CN^- ions substituted for the halogen in KCl, KBr, KI, RbCl, NaCl and NaBr. Energy levels associated with the ion performing free rotation, hindered rotation, oscillation and tunneling motion were observed. A free molecule containing *N* atoms has 3N-6 degrees of vibrational freedom, three degrees of translational freedom and three degrees of rotational freedom. When a molecule is introduced substitutionally into a lattice, the vibrational degrees of freedom are usually changed relatively small by the matrix.

The translational degrees of freedom of the molecule are the same as the translational degrees of freedom of an impurity atom, i.e., they manifest themselves as impurity modes. We have considered the third group of degrees of freedom, those connected with the rotational inertia of the molecule. The present study originated from the study of phonon defect interactions through measurements of the low- temperature lattice thermal conductivity initiated by Sproull and co-workers. Klein[1] noticed that NaCl crystals grown in air had an extremely low thermal conductivity of a very peculiar temperature dependence. He was able to relate this phonon scattering to some molecular impurities which absorbed light of 186 mμ wavelength. This defect has since been identified by him as the OH^- ions[2].

Klein expected that the strong phonon scattering was associated with the rotational degrees of freedom of the impurity ion. The study of these defects and their interactions with the phonons was complicated due to the fact that he could

not detect the OH^- ions in NaCl by IR spectroscopy. In KCl, the infrared O-H stretching vibration was extremely weak[3].

The reason for this influence of the host lattice is still unknown. The small dipole moment observed in the IR absorption is in striking contrast to the result obtained in the dielectric measurements where a dipole moment $\mu \sim D$ was found. Taking the Klein's suggestions into account we have studied CN^- in a number of alkali halide host lattices. These molecules show infrared absorptions of the theoretically estimated strength. Thus, it appears that the trapping of the molecule ion in the lattice vacancy does not affect its vibrational properties to a great extent. We wish to show how a combined use of photon and phonon spectroscopy and of specific heat measurements can yield a detailed picture of the rotational degrees of freedom of molecular ions in solids and of their phonon scattering cross- sections. This chapter deals with CN^- ions which is particularly a simple case one. On the other hand, the more complicated NO^-_2 ion gives a deeper insight into the variety of rotational and translational degrees of freedom which are possible for a molecule in a solid in the most general case.[4-10]

1.1.1 Experimental Techniques:

Almost all infra-red measurements between 2.5 μ and 15μ were made with a Beckman IR-7 prism-grating spectrometer with NaCl optics. It is primarily designed for double beam operation at ambient temperatures. In order to make measurements at low temperatures with small samples the spectrometer was modified, so that the beam having passed through the monochromator, was focused on to the sample.

The cross- section of the beam striking the sample, the cross- section varies slightly with wavelength since the slit width is varied with wavelength, was 1cm×0.01 cm. at 2100 cm^{-1} instead of 2.5cm ×0.6cm. when placed in the usual

compartment of the IR-7. The use of monochromatic light also reduces the radiation heating of the sample and avoids a possible radiation induced change in population of the energy states of the molecule. The resolution obtained at low temperatures was 0.3 cm^{-1} between 1000 cm^{-1} and 1300 cm^{-1}, and 0.6 cm^{-1} at 2100 cm^{-1} Measurements between 2.0μ (5000 cm^{-1}) and 2.45μ(4000 cm^{-1}) were made with a Cary Model−14 spectrometer. Its resolution was approximately 5×10^{-3}μ (1 cm^{-1}).

Measurements above 4.2^0K were made with conduction cryostats of conventional design. The use of LiF cold windows mounted on the liquid N_2 radiation shield decreased the lowest temperature obtained from 13 to 7^0K. Higher temperature measurements were made during the warm up. Temperature measurements were made with 1000− and 1500 $-\Omega\frac{1}{10}-W,$ calibrated Allen Bradley carbon resistors. These resistors were calibrated against a gas thermometer in the Cornell thermal conductivity equipment. Measurements below 4.2^0K were made with an immersion cryostat.

The difficulty is to make a seal between an infra-red transmitting window and the helium chamber which does not crack upon cooling and is tight to super fluid helium. A similar technique for an exchange gas cryostat has been described by Roberts. [11]

Fig. 1.1 shows an expanded view of the window arrangement A 1-in diam circular CaF_2 window was epoxies to a well annealed 3-mil copper diaphragm with Hysol 4314 epoxy resin. The diaphram was soldered with Wood's metal to the copper liquid-helium can. The most successful pair of windows has been cycled to λ helium temperatures more than 100 times and is still in use. The least successful pair was cycled only twice. For measurements out to 13.5 μ, Irtran-2 windows were used. KCl and KBr windows were also tried but were unsuccessful. With

and without 'Cold' LiF windows on the nitrogen radiation shield, the lowest temperatures attained in the cryostat were 1.36 and 1.55^0K, respectively. The temperature of the bath was measured with a 56Ω calibrated Allen- Bradley resistor. The temperature difference between the crystal and the bath is estimated to less than 0.01^0K. With the LiF 'Cold' windows the bubbling of the normal helium was sufficiently small to enable steady-state measurements to be made at 4.2^0K. For measurements between the λ point and 4.2^0K, the bath was first pumped to a temperature below the desired temperature. A pressure gradient was then set up along the length of the helium path by closing the valves to the helium pumping system. Once the desired temperature was reached, the temperature was maintained for long periods of time with very little bubbling of the He bath by pumping through a $\frac{1}{8}$ in needle valve.

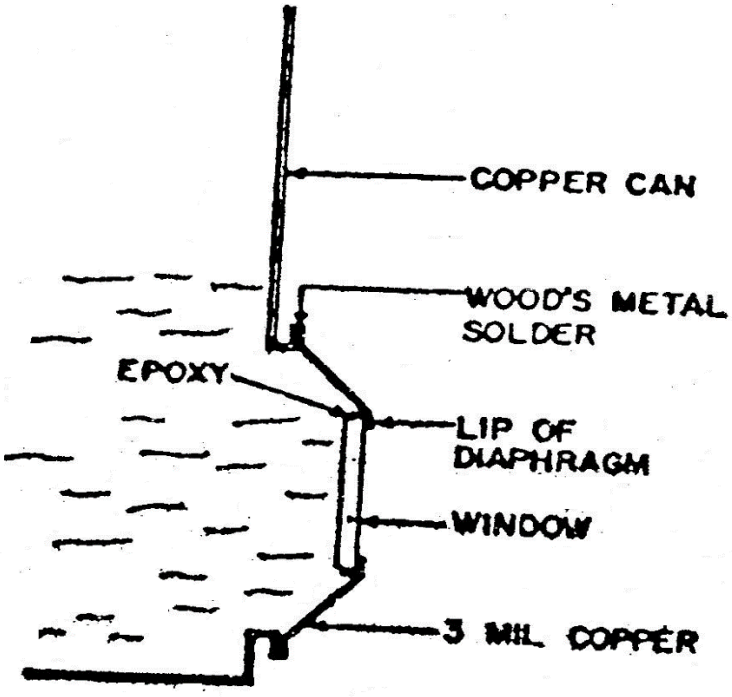

Fig. 1.1. Schematic of the window arrangement used in the immersion cryostat.

The immersion cryostat was also used for studying changes in the CN^- absorption spectrum under the influence of a static electric field or uniaxial stress. For electric fields parallel to the direction of the incident light nickel meshes (50 lines/in) were used as electrodes. An electric field perpendicular to the direction of the incident light was applied by means of metal electrodes.

For the uniaxial -stress measurements the crystals were mounted on a slotted cylinder to allow passage of the IR beam. The stress was applied perpendicular to the direction of the incident beam with a hydraulic pump. In order to obtain uniform strain, J oil was applied to the crystal surfaces. Several stress runs were made, and the data presented represent an average of all the runs.

1.2 Measurement of The Thermal Conductivity:

The thermal conductivity was measured using the standard steady- state method in a He^4 cryostat[12,13] and in a He^3 cryostat that was built for measurements between 0.3^0 and 2.0^0K. Fig. 1.2 is a cross- section of the experimental chamber of the He^3 cryostat showing the position of the sample. Thermal contact to the crystal was made with indium-faced phosphor bronze clamps. The thermal gradient along the crystal was measured with speer $\frac{1}{2}-W,470\Omega$, grade 1002 carbon resistors which were calibrated in each run. After 10-15 runs the speer resistors would become noisy below 0.5^0K and had to be replaced by a fresh pair.

The primary temperature standard was a Honeywell germanium resistance thermometer, which had been initially calibrated using He^3 He^4 vapour pressure thermometers and a paramagnetic salt thermometer.

All resistance measurements were made with an A.C. Wheatstone bridge having a maximum sensitivity for a 5000–Ω resistor of 1 part in 10^4 while only dissipating 10^{-10}W in the resistor.

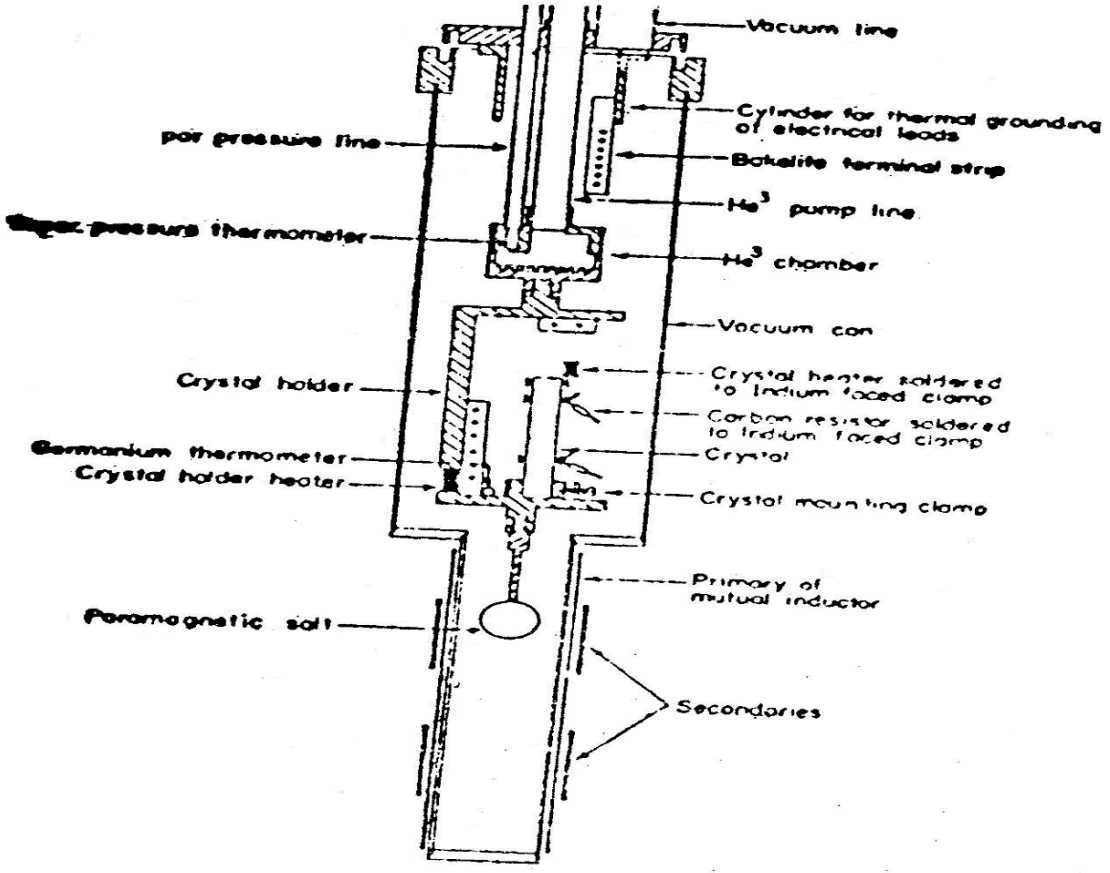

Fig. 1.2 Cross-sectional view of the experimental chamber of the He^3 cryostat.

1.2.1 Specific Heat:

The specific heat sample of mass 4 to 31g was cemented to a 0.3×0.4×1.0cm support of either graphite or KCl heavily doped with KCN which was clamped to the crystal holder of the He^3 cryostat.

The thermometer, a $\frac{1}{10}W$, 10 –Ω Allen-Bradley resistor and a 1000– Ω Nichrome wire (0.025mm) heater were secured to the crystal with varnish. A support with very low thermal conduction was necessary so that heat put into the crystal would leak out sufficiently slowly to allow the change in temperature and hence the specific heat to be measured.

The time constant for the sample to approach the bath temperature was always at least 20 times longer than the duration of the heat pulse and the response time of the thermometry. The validity of the technique was tested on pure KCl whose specific heat was found to be proportional to T^3 with a Debye θ of 229 ± 2^0K compared to 233 ± 3^0K as given by Kelsom and Pearlman.[14]

1.2.2 Crystals:

The crystals were pulled from the melt in the crystal growing facility of the Material Science Centre at Cornell from halogen treated analytic reagent- grade material to which the proper amount of dopant had been added, using alumina, platinum or pyrolytic graphite crucibles and purified argon as protective atmosphere. The crystals were about 10 cm long and 1.5cm in diameter and clear except for the highest doping (0.5 mole % in the melt) which shows signs of precipitation at the bottom. These portions were discarded. For the spectroscopic determination of the CN^- concentrations, we refer to table 1.1.

In the infra-red the only impurity within the limit of detectability was NCO^-. In the ultraviolet rudimentary "OH" bands were found. In the 0.5 mole % CN^- doped crystals the absorption co-efficient of this band was of the order of 1 cm^{-1} in all the alkali halides.

Table-1

Host lattices	$\upsilon_{CN^-}(cm^{-1})$	σ_{CN-} (cm^{-2})
KCl	2105	3.6×10^{19}
KBr	2097	3.1×10^{19}
KI	2067	6.7×10^{19}
NaCl	2104	1.8×10^{19}
NaBr	2086	1.55×10^{19}
RbCl	2075	5.2×10^{19}

Spectroscopic determination of CN^- concentration. The concentration $N_{CN^-}(cm^{-2})$ is related to the peak absorption coefficient α_{CN-} are given in the table together with the frequency υ_{CN-} of the CN^- stretching fundamental for the different alkali halides at room temperatures.

The constant σ was determined for each host lattice from a chemical analysis performed at the Analytical Facility of the Cornell Materials Science Center. The chemical determinations are believed to be good to 10% for the alkali halides expecting KI and RbCl, which are good to 30%.

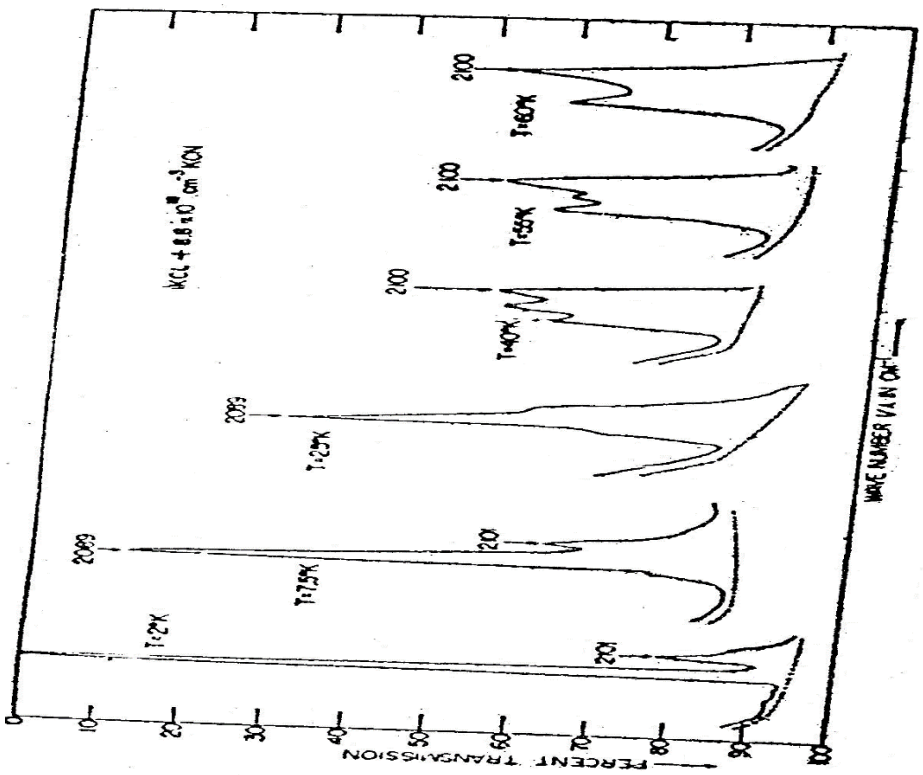

Fig. 1.3 Transmission spectra of 5mm thick KCl crystal Containing $8.8\times10^{18}cm^{-3}$ CN^- ions.

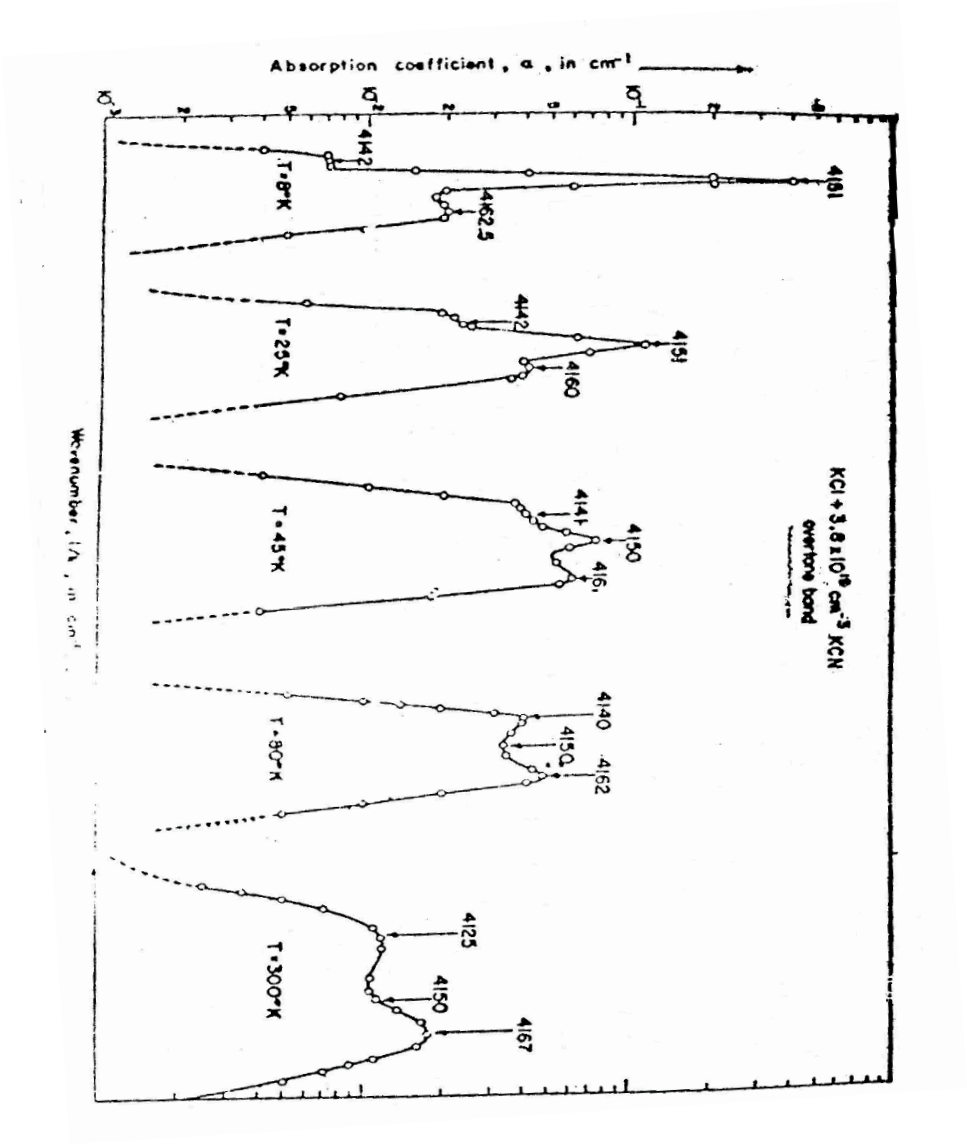

Fig. 1.4 Absorption spectra of the CN^- overtone vibration in KCl.

In the pure samples, this absorptions was of the order of 0.1 cm^{-1} or less. The origin of the ultra violet absorption band in cynide-doped alkali halides has been ascribed to NCO^- by Akpinar[15] and to OH^- by Rolfe et.al.[16].

The thermal conductivity measurements indicate that the ultra violet absorption in our doped crystals probably not due to OH^-. Our thermal conductivity results for NaCl + NaCN show no low temperature scattering whatsoever. Klein found a strong phonon scattering for NaCl doped with NaOH.

The absorption coeffcient was~1 cm^{-1} at 190mμ for thermal conductivity crystal. From ionic conductivity measurements on KCl containing 4×10^{19} cm^{-3} CN^- between 200 and 400^0 C it was concluded that the vacancy concentration was the same as in our undoped crystals i.e., at most ppm. This is as expected for the singly charged CN^- ion sitting in a substitutional site. On the other hand, doping with negative ions like OH^-, CO^-_3 SO^-_4 has been found significantly affect the ionic conductivity due to association either with positive divalent ions or vacancies[17-19]. In summary it may be said that in our crystals the primary impurity other than CN^- is the NCO^-. Infrared and ionic conductivity measurements indicate that the absorption in the cynide stretching region is due to the singly charged CN^- ion in a substitutional site. The size of the samples used for the low-temperature infrared measurements varied from 0.5 to 12mm in thickness and usually had a cross-section of $1cm^2$. The stress samples were usually 3.5×3.5×12mm with the long axis being the direction of uniaxial stress. The electric field samples were between 0.5 to 1mm thickness and $1cm^2$ in cross-section. The field was applied along the small dimension. The thermal conductivity samples were 5×5×40mm in size except samples for electric field measurements which were 6×2×40mm. Electric fields were applied with evaporated gold electrodes 500-100-A^0 thick. The surfaces of the Cleaved crystals were sand- blasted in order to ensure diffuse phonon scattering by the boundaries.

1.2.3 Absorption Spectra:

In Fig. (1.3) and (1.4) we compare the spectrum of the fundamental and the overtone vibration of CN^- in KCl. Their features are almost identical. At 2^0K the spectrum consists of a central line at 2089 ± 1 cm^{-1} (4151cm^{-1} for the overtone) with a weak sum satellite 12 ± 1 cm^{-1} away. At about 8^0K a weak difference satellite arises. It is less well resolved, and its

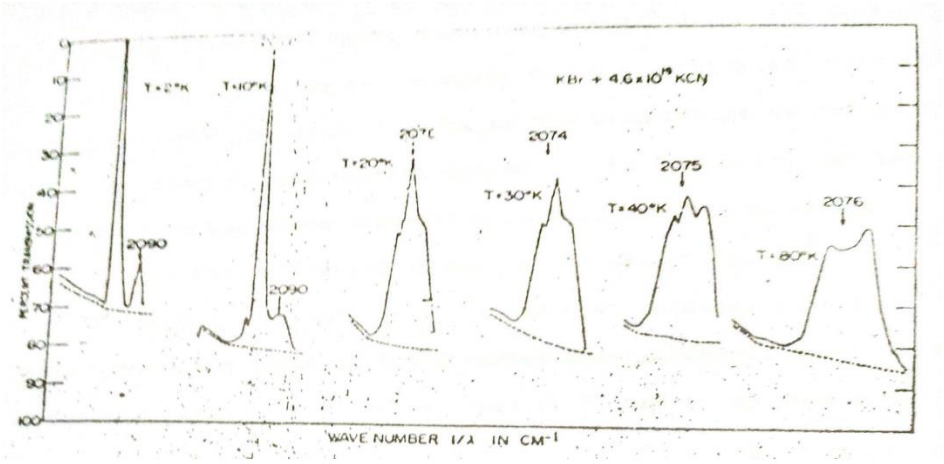

Fig. 1.5: Transmission spectra of 16mm. thick KBr crystal containing 4.6×10^{19} cm^{-3} CN^- ions.

separation is 8 ± 2 cm^{-1} (9 ± 2 cm^{-1} for the overtone). At T=25^{0}K the central peak's intensity decreases while the sum and difference satellites increase in intensity and the satellites shift in position toward the central peak. As the temperature increases to 40^{0}K, the central peak further diminishes in intensity, but two broad bands arise whose separation increases with increasing temperature. The separation of the broad bands is 23 ± 1.5cm^{-1} at 80^{0}K and 40±2.5cm^{-1} at 295^{0}K for both spectra. At all temperatures the width of the observed absorptions is not limited by the instrumental resolution.

Figs. (1.5) and (1.6) show the spectrum of CN^- in KBr for the fundamental and overtone vibrations. A weak sharp line at 2074 cm^{-1} which is probably due to NCO^- has been subtracted from the spectrum in fig (1.5) definitely not due to CN^- since it was not observed in the overtone spectrum. Obviously here again the separation of the sum satellite from the central line is about 12cm^{-1}. The only differences betwee the KBr and KCl spectrum are that at high temperatures the central minimum is not so deep and that the separation between the broad bands at higher temperatures is slightly smaller, 20 ± 1.5 cm^{-1} at 80^{0}K and 35 ± 5cm^{-1} at 295^{0}K.

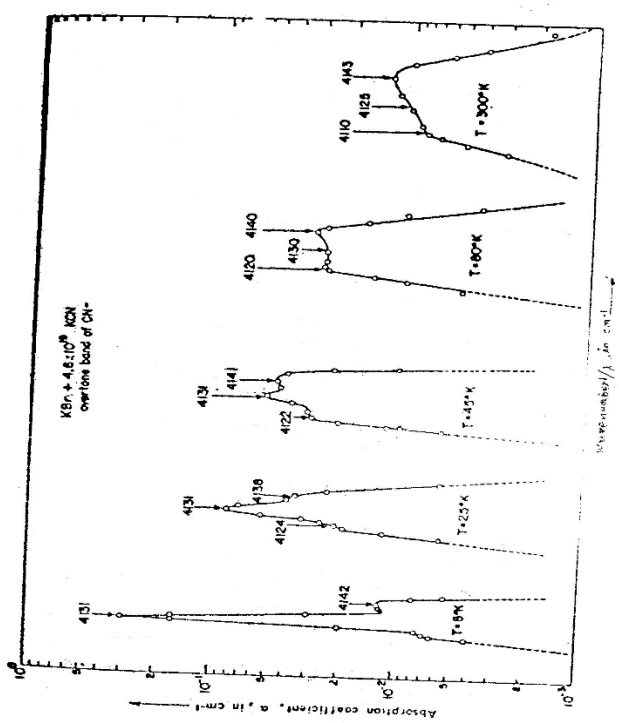

Fig. 1.6: Absorption spectra of KBr+4.6×10^{19} cm^{-1} KCN overtone vibration of CN^{-}

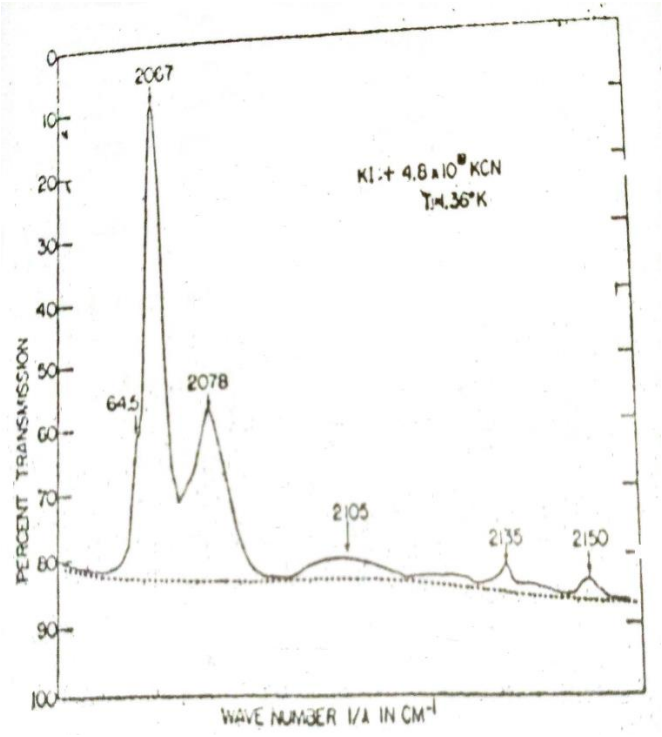

Fig. 1.7: Transmission spectra of 3mm KI crystal containing CN^{-} ions at 1.36^{0}K.

The striking identity of the structure observed with fundamental and overtone vibrations proves that this structure is not merely the result of having the vibrational energy of some of the CN^- ions different from the majority because of different surroundings like clusters, interstitials etc., If this were the case, the structure of the overtone absorption would have twice the width of the fundamental. Rather the structure is caused by a simultaneous excitation of the stretching vibration, with $\Delta\upsilon = 1$ for the fundamental and $\Delta\upsilon = 2$ for the overtone, plus or minus some other transitions, interpreted as librational or rotational ones.[7]

Fig. (1.7) shows the CN^- spectrum in KI at 1.36^0K. Fig (1.8) shows the spectrum for higher temperatures. At T = 1.36^0K one again observes a central line with a weaker sum satellite about 11 cm^{-1} away and a barely resolvable difference satellite approximation 2.5 cm^{-1} away at 2064.5cm^{-1}. In addition, broad bands are observed with maxima at approximately 2110, 2135, and 2150cm^{-1}, i.e. 43cm^{-1}, 68cm^{-1} and 83cm^{-1} from the main CN^- line at 2067cm^{-1}. At higher temperatures the spectrum is very similar to that observed in KCl and

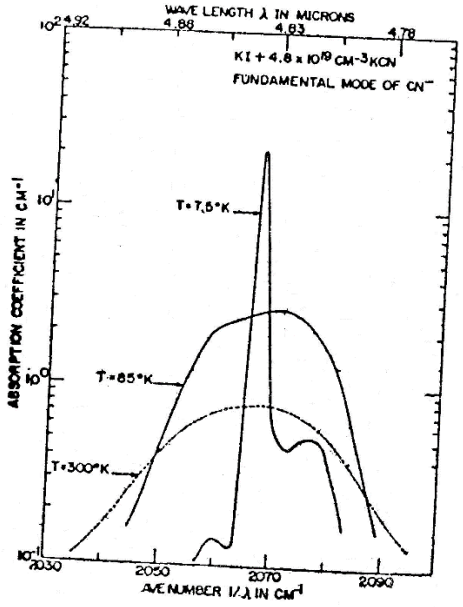

Fig. 1.8: Absorption spectra of KI+4.8×$10^{19}$$cm^{-3}$ KCN. Fundamental vibration of CN^-.

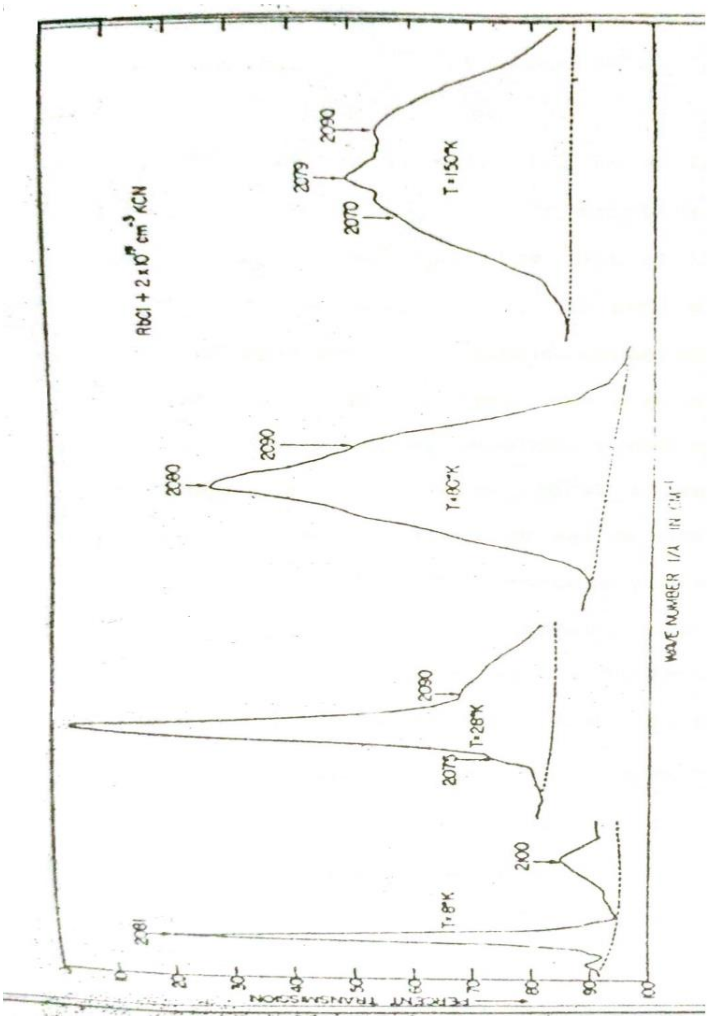

Fig. 1.9: Transmission spectra of 3.5mm RbCl. crystal containing $2\times10^{19}cm^{-3}$ CN^-ions.

KBr except that now the central minimum is no longer detectable. The half - width of the observed broad band is 22 ± 1 cm^{-1} at 80^0K and 40 ± 2 cm^{-1} at 295^0K.

The CN^- spectrum in RbCl is qualitatively similar to that in potassium salts, but the splitting of the sum satellite is now larger, $19cm^{-1}$, and the central line disappears only at about 150^0K shown in fig. (1.9).

In NaCl and NaBr the spectrum consists of only one narrow band whose half-width is proportional to the square of the temperature as shown in figs. (1.10) and (1.11).

The instrumental resolution did not allow the determination of the line shape below, 80^0K. A weak low- energy satellite $4cm^{-1}$ away from the main line was observed in NaCl and NaBr at low temperatures.

With the overtone vibration a low- energy satellite 8 cm^{-1} away was observed. This suggests that these lines are to be associated with a different center, possibly CN^- in a different position in the lattice.

1.2.4 Electric-Field and Stress Effects:

The effect of a static electric field on the CN^- infrared absorption in KCl:CN and NaCl: CN was studied at 2^0K. The field was applied in [100] and [110] direction and was oriented both in the direction and perpendicular to the direction of the incident polarized light beam.

For a maximum field of 80KV/cm, the observed change in optical density was less than 5%. Under the assumption that the CN^- dumbbell carriers a permanent moment μ like a classical dipole, we conclude that the molecule is either frozen-in at 2^0K or that μ is small.

A distinction between these two possible explanations was achieved through uniarial stress experiments.

The observed change in optical density of the infrared band gives a direct measure of the number of molecules oriented parallel to the stress, axis, denoted by N_{II} and the number oriented perpendicular to the stress, denoted by N_{per}.

Stress alignment was found in KCl, KBr, KI and RbCl.

Fig. (1.12) shows the directional dependence of the alignment at 1.36^0K as a function of stress for KCl

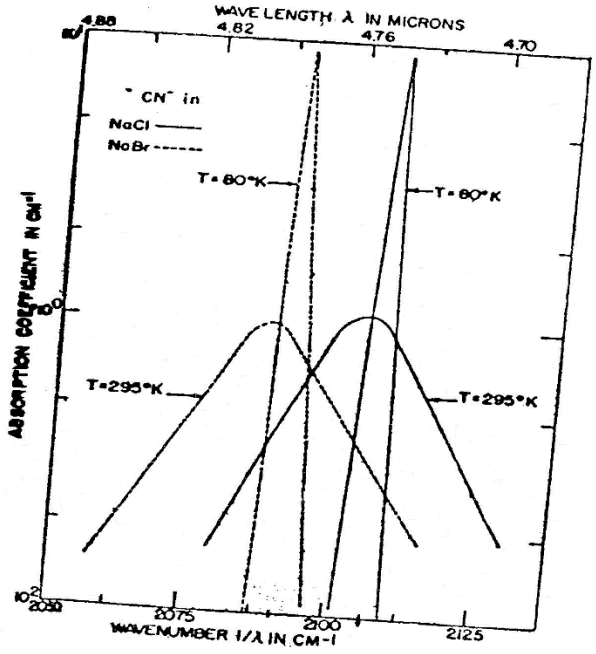

Fig. 1.10: Absorption spectra of CN^- fundamental vibration. Solid lines NaCl+2×10^{19}cm^{-3} NaCN, dashed lines NaBr 1.6×10^{19}cm^{-3} NaCN.

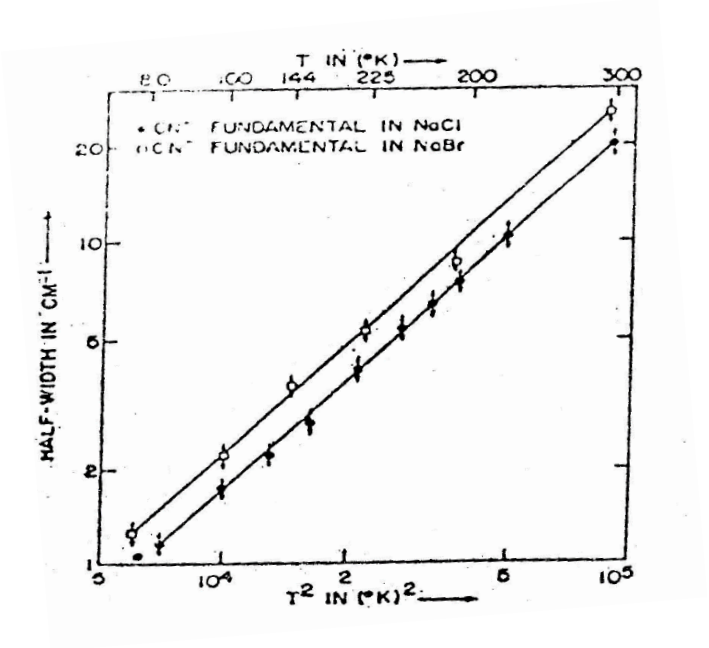

Fig.1.11: Half-width of CN^- fundamental vibration as a function of temperature. Upper line: NaBr+1.6 ×10^{19}. cm^{-3} NaCN, lower line: NaCl+2×10^{19}cm^{-3} NaCN.

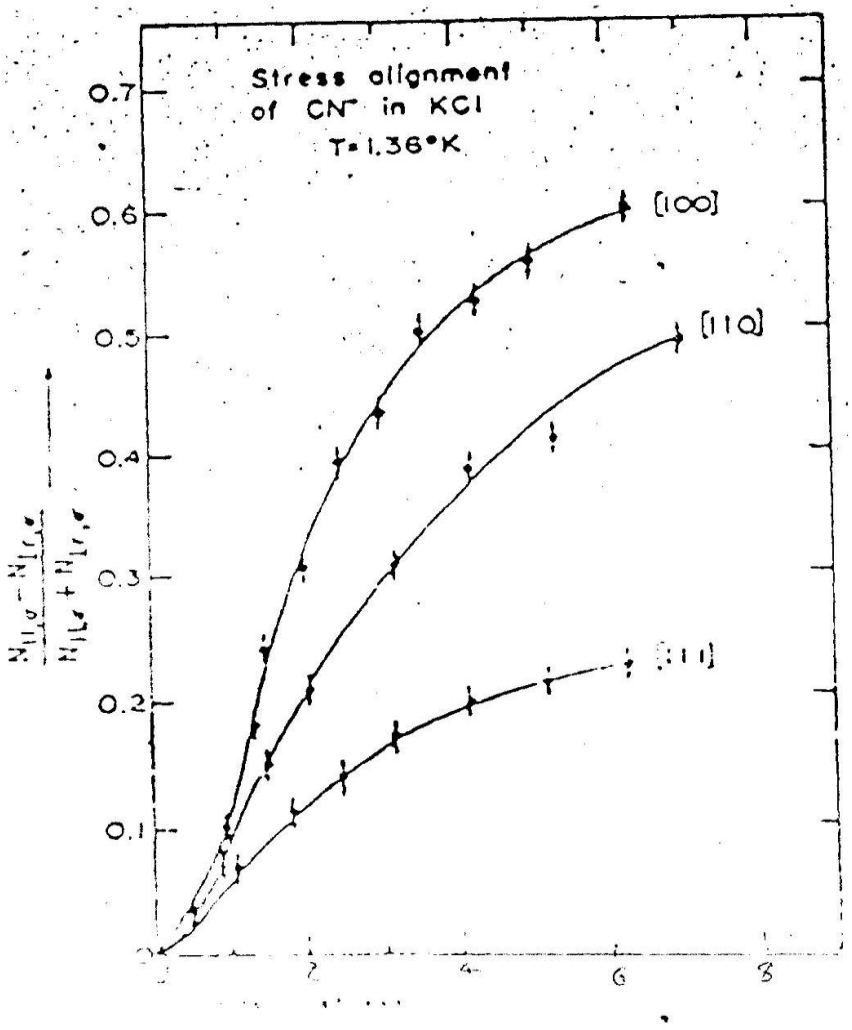

Fig. 1.12: Alignment of the CN^- ions as a function of uniaxial stress.

Fig. (1.13) shows the temperature dependence of the alignment between 1.36 and 4.2^0K. It can be seen that for moderate stresses the alignment follows a 1/T law. The alignment observed in other host lattices is smaller. Fig. (1.14) shows the results for [100] stresses in KCl, KBr, KI and NaCl. It can be seen from the figure that no alignment is observed in NaCl and NaBr. This was studied between 1.36 and 4.2^0K and for the [100] and [110] stress directions. After applying the uniaxial stress it is observed 10 to 5 min and failed to detect any alignment in these two host lattices and the same results were obtained for NCO^- in KCl, KBr and KI. In all the other host lattices the alignment followed the stress within the time constant of the instrument.

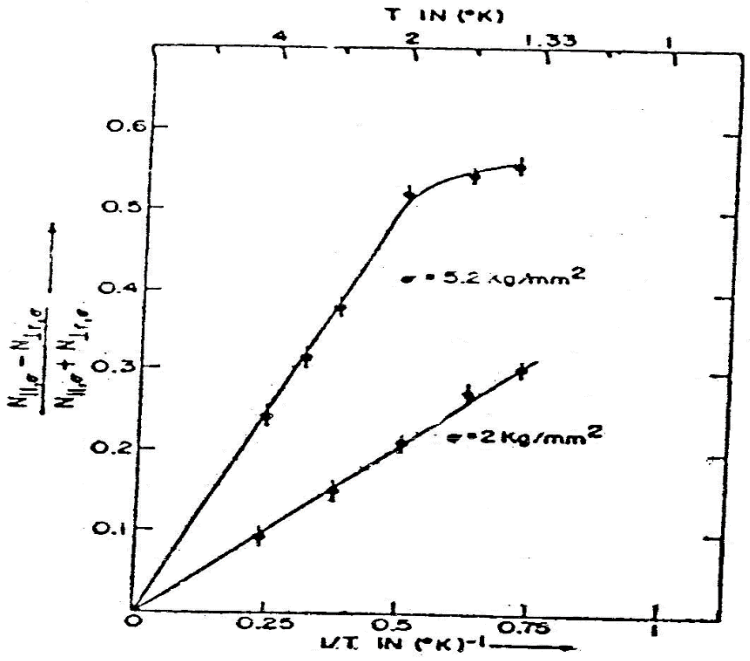

Fig. 1.13: Temperature dependence of the CN^- alignment in KCl for [100] uniaxial stress. Upper curve σ =5.2kg/mm^2, Lower curve σ = 2kg/mm^2.

1.3 Theory:

Molecules in crystalline environments are expected to have discrete equilibrium orientations. Most of the features observed with CN^- in alkali halides can be explained with a simple two-well cosine potential. There- after we shall discuss how a quantitative description can be obtained by using a more realistic three dimensional potential of octahedral symmetry.

Following Pauling we choose a potential of the form.

$$V = \frac{V_0}{2}(1 - Cos2\theta) \quad \text{..... (1.1)}$$

The Schrodinger equation for this potential is known as Mathieu's equation and can be solved exactly.

When $KT << V_0$, the molecules occupy energy states below the top of the barrier. In the harmonic approximation these energy levels correspond to those of a harmonic oscillator.

Figure

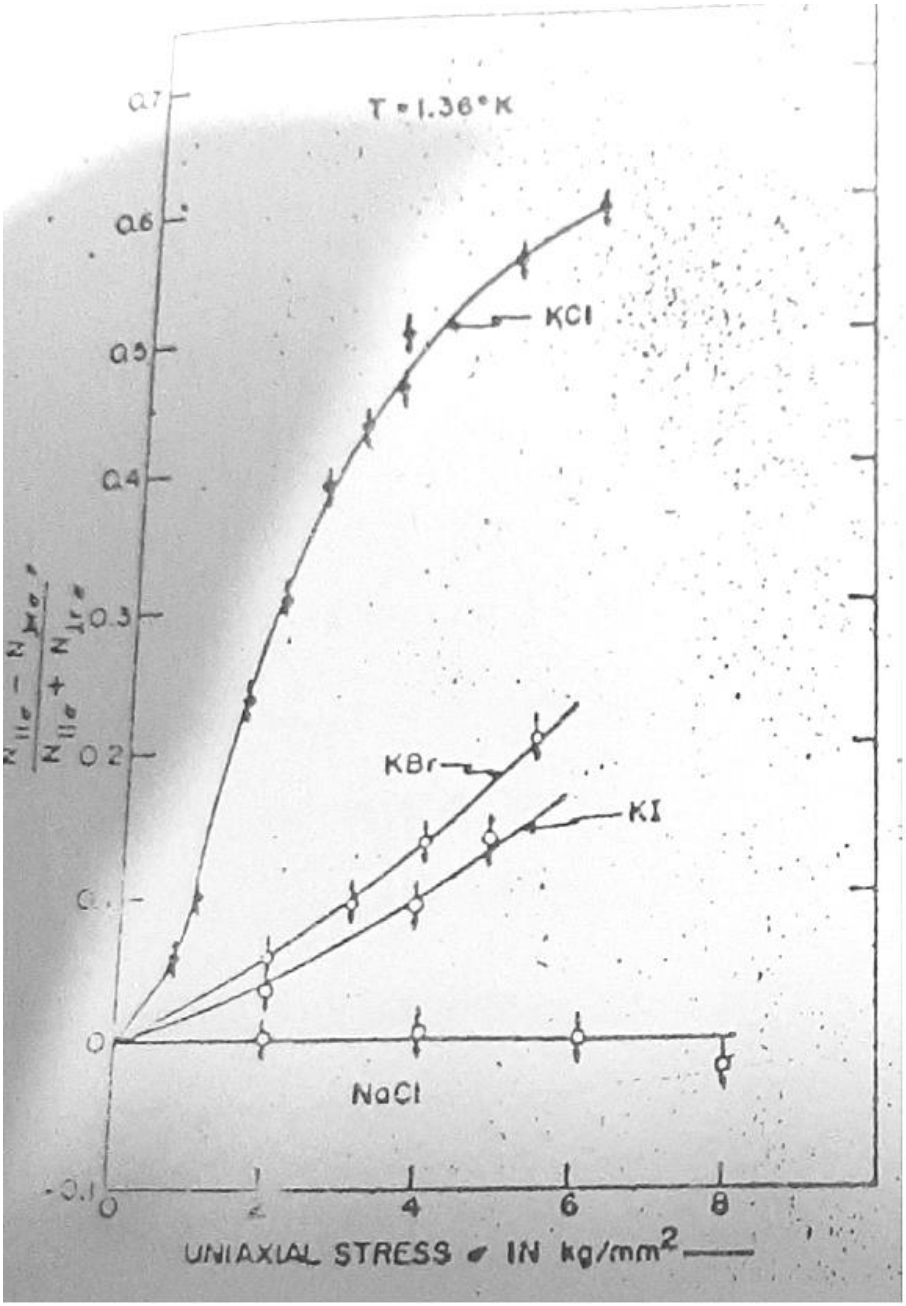

Fig. 1.14: Alignment of CN^- in different host lattices with [100] uniaxial stresses at T = 1.36^0K.

$$hc\tilde{\nu}_n^{lib} = hc\tilde{\nu}_0^{lib}\left(n+\frac{1}{2}\right) \text{.....(1.2)}$$

with

$$\tilde{\nu}_0^{lib} = 2\left(\tilde{V}_0\tilde{B}\right)^{\frac{1}{2}} \text{.....(1.3)}$$

Where $\tilde{\nu}_0^{lib}$ is the fundamental librational frequency in cm^{-1} and $\tilde{B} = h/8\pi^2 CI$ is the rotational constant in cm^{-1}. All the quantities marked with ~ are in cm^{-1}. 1 cm^{-1} correspondence to $E = 1.24\times10^{-4}$ ev and $f = 3\times10^{10}$ $Sec^{-1} = 1.42^0K$. Each energy level of the harmonic librator is two fold degenerate for $\tilde{\nu}_0^{lib} << \tilde{V}_0$. In reality these levels are split due to the possibility of quantum-mechanical tunneling through the barrier.

The selection rules for the degenerate librator have been worked out by Hexter and Dows.[21] They showed that in the near-infrared vibrational spectrum the strongest transitions involve no changes in the librational quantum number, i.e., they give rise to the transition $\Delta n = 0$ which is called the *Q* branch. Because of anharmonicity, weaker transitions $\Delta n = \pm 1, \pm 2,$ .....etc. are allowed. These give rise to a succession of equally spaced lines which decrease in intensity by the factor.

$$\left(\tilde{\nu}_0^{lib}/2\tilde{B}\right)^{\Delta n}.$$

In addition, the different transitions are weaker than the sum transitions by Boltzmann factor.

The eigenstates with energies large compared to V_o corresponed closely to those known for free molecules. We use the term "free rotations' for the case in which most of the moleculas occupy energy states lying above the barriers. The free torator energy levels are given by

$$\tilde{\upsilon}^{Rot} = \tilde{B}J(J+1)$$

Where J is the rotational quantum number. Each level is (2J+1) fold degenerate. The selection rules for the vibrating rotator are $\Delta J = \pm 1$. The transitions with $\Delta J = +1$ and $\Delta J = -1$ give rise to the R and P branches respectively, while the transitions with $\Delta J = 0$ (the Q branch) are now forbidden. The Q branch is forbidden only in the case of diatomic molecules. This makes it particularly easy to detect the transition from librational to rotation for such molecules. For more complicated molecules the Q branches are generally allowed thereby making the interpretation more dfficult.

The shape of the vibration- rotation band is determined largely by the thermal polution of the rotational levels. If one assume that the intensity of the transitions from a given rotational states J is governed solely by the number of molecules in the state J, then the separation of the maxima in the P and R branches is given by[22]

$$\Delta\ \tilde{\upsilon}_{PR}^{\max} = \left(8\tilde{B}kT/hc\right)^{\frac{1}{2}} \propto T^{\frac{1}{2}} \quad \text{.....(1.5)}$$

The results of the above simple theory may be briefly sumarised as follows:

At low temperatures ($kT<<V_0$) the infrared spectrum should consist of a strong Q branch with weak satellites separated from the fundamental by multiples of the libration frequency, $\tilde{\upsilon}_0^{lib}$. At high temperatures ($kT>>V_0$) the spectrum should approximate that known for free molecules, i.e., it should consist of P and R branches with a missing central Q branch. For Intermediate temperature ($kT\approx V_0$) the spectrum should consist of P, Q and R branches of comparable intensity.

Let us supplement this quantum mechanical discussion of the states of vibrational motion with the semi-classical picture of a rotating molecule. One can describe the states below the barrier V_o as oscillatory motions of the molecule in a particular well.

This does not simply mean however, that in these states the molecule cannot move from one well to the other. These states are therefore, frequently called states of hindered rotation or states of almost free rotation. Such a change of the orientation is of particular interest if the influence of an electric or a stress field is studied. We can then describe the orientation as a thermally activated rate process, involving a classical jumping of the molecule over the potential barrier with a jump rate υ_{jump}.

$$\upsilon_{jump} = \upsilon_0^{lib} \exp\left\{-\left(V_0 - \frac{1}{2}h\upsilon_0^{lib}/kT\right)\right\} \quad \text{..... (1.6)}$$

It must be noted that this description fails if the reorientation takes place through a tunnel process which is purely quantum mechanical.

1.4 Comparison with Experiment:

A qualitative comparison of the KCl and KBr data with the selection rules stated above indicates that at low temperatures, below 20^0K, the motion of the molecule can best be described as libration. Between 20^0 to 50^0K the molecule performs hindered rotational motions, i.e., in this temperature region a significant number of molecules occupy energy states both above and below the barrier. Above 60^0K most of the molecules occupy energy states lying above the barrier and now the characteristic P and R maxima of free molecules are observed. Fig. (1.15) shows that the separation of the P and R maxima follows a $T^{\frac{1}{2}}$ law as predicted by equation (1.5). From these data the rotational constant $\tilde{B}$=1.25cm^{-1} is obtained for the KCl host lattice.

The error in determination $\tilde{B}$ by this method is determined by the width of the P and R maxima and is estimated to be about 20%. From $\tilde{B}$ the moment of inertia I and hence the inter-nuclear separation between the C and N atoms is calculated to r = 1.4A^o for KCl. For KBr one gets a smaller value of $\tilde{B}$(1.0 cm^{-1}). The P and R branches are not as clearly resolved in KBr as in KCl which is probably due to center-of mass motion of the molecule. The value of 1.25cm^{-1} found in KCl will be assumed to be true $\tilde{B}$ value for all host lattices.

Pauling[23] has estimated the radii of the carbon and nitrogen atoms for the C-N bond length may be deduced. Recently Elliot and Hastings[24] have used 1.16A^o for the C-N bond length in pure KCN in order to fit their neutron-diffraction data. Considering the simplicity of the model used here the agreement between calculated and experimental values is considered very satisfactory.

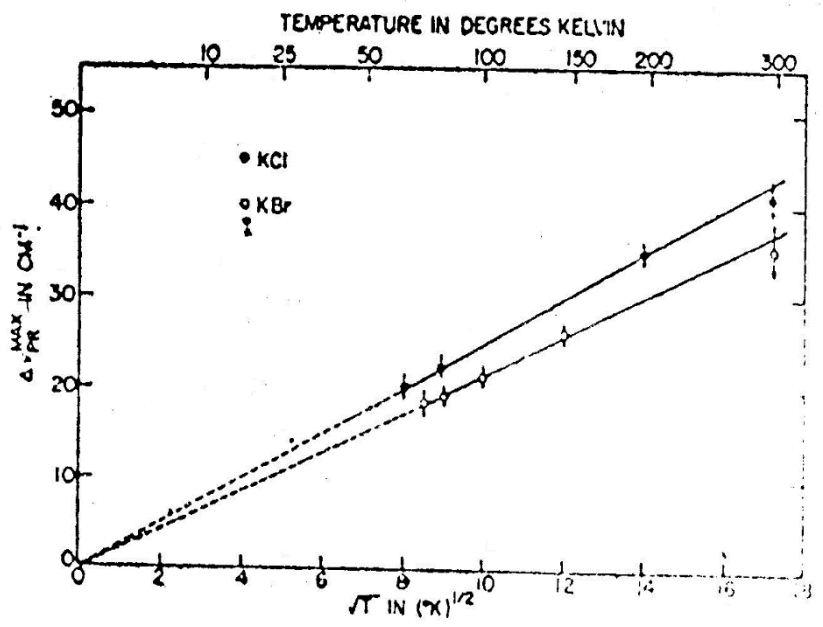

Fig. 1.15: Separation of the P and R maxima in cm^{-1} as a function of temperature. Upper line: KCl +8.8×10^{18} cm^{-3} KCN; lower line KBr+4.6×10^{19} cm^{-3} KCN.

It follows from above that the motion of the CN^- in KCl and KBr is very nearly free at 60^0K and above. Therefore the barrier height must be less than 40cm^{-1}. From Pauling's model the barrier height can also be determined directly from the librational frequency on the basis of equation (1.3). One obtains $\tilde{V}_0 \approx 24 cm^{-1}$. The zero point energy of the librator is 6cm^{-1} and hence the first librational state lies just below the barrier. The energy states above the barrier should approximate the free rotor levels closely. The rotational fine structure (Separation = $2\tilde{B} \approx 2.5 cm^{-1}$) has not been observed.

The above interpretation of the CN^- fundamental spectra in KCl and KBr is completely confirmed by the data for the CN^- overtone vibration in these host

lattices. The overtone vibration shows a $12cm^{-1}$ librational satellite at low temperatures and characteristic P and R maxima at high temperatures whose separation is the same, within the experimental error, as that observed for the fundamental. The identity of the spectra for the fundamental and overtone vibrations indicates (1) that the interaction between vibration and rotation is negligible for the CN^- molecule and (2) that the barrier hindering rotation is independent of the vibrational state i.e., vibrational polarization effects are unimportant in determining the barrier hindering rotation. This conclusion is evident also from the fact that the Q-branch frequencies change from host lattice to host lattice without bearing any obvious relation to the potential barrier hindering rotation. The barrier appears to be insensitive to the halide ion but very strongly dependent on the nearest neighbour alkali ion. The reason for this are unknown but experimentally the stress effects show that the CN^- dipole prefers to point towards the nearest neighbour alkali ion.

In RbCl the librational satellite is $19cm^{-1}$ away so that $\tilde{V}_0$ for the two fold potential is about 60 cm^{-1}, i.e., the barrier height is about $2\frac{1}{2}$ times that in KCl or KBr. This is confirmed by the temperature dependence of the spectra in RbCl which show P and R maxima only at very high temperature, less than 150^0K, with a very weak active Q-branch.

The spectra of CN^- in KI is similar to that observed in KCl and KBr at low temperatures. At high temperatures, however, the P and R branches are not resolved. Instead one obtains a broad absorption band of a width proportional to

$T^{\frac{1}{2}}$ as shown in fig. (1.16). These data closely resemble the data for the separation of the P and R maxima in KCl shown in fig. (1.15). One might have expected a clear resolution of the P and R maxima in KI because the I^- cavity is large and hence the barrier to rotation should be low. Yet there appears to be some mechanism disturbing the free rotation at high temperatures and causing the Q-branch to become allowed. The selection rules for the librating molecule prefer the Q-branch[21]. Similarly we suspect that for a molecule performing translational oscillations the Q- branch may become allowed. Evidences for such a motion is given by the high- energy satellites observed at low temperature, spaced 40,68, and 83 cm^{-1} from the main band. They may be caused by either of the following two mechanism:

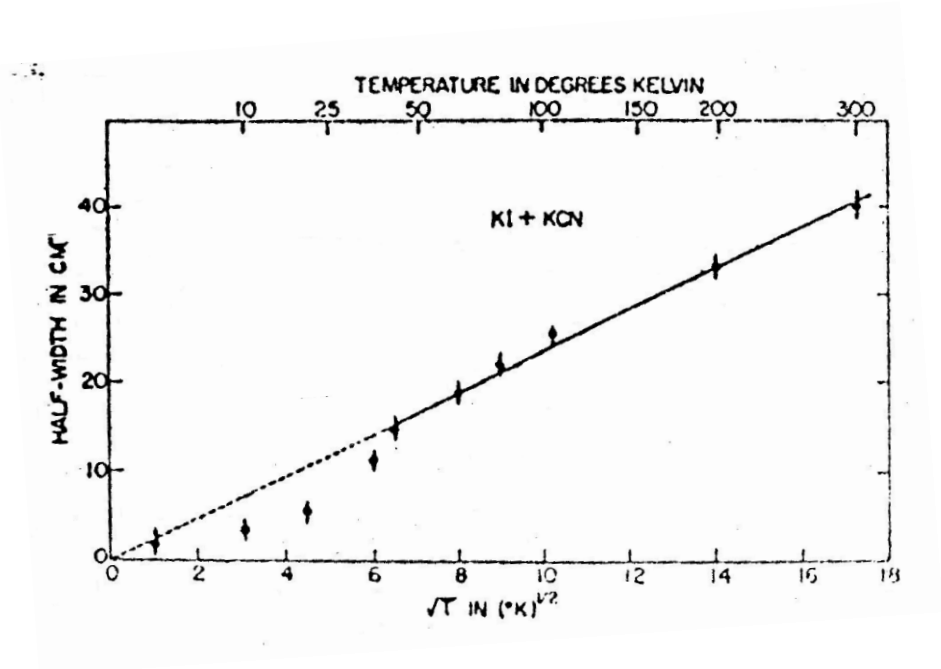

Fig. 1.16: Half- width of CN^- fundamental absorption in KI as a function of temperature.

The 40-cm^{-1} satellite may be associated with a resonant mode and the other two, narrower bands may be caused by excitations of local modes in the gap.

Since the CN^- ion possesses symmetry $C_{\infty\upsilon}$ two transitional local mode of symmetry A_1 and E_1 should be allowed, the A_1 mode corresponding to transitions along the inter-nuclear axis and the doubly degenerate E_1 mode corresponding to transitions along axes perpendicular to the inter-nuclear axis. In recent far-infrared absorption measurements Lytle and Sievers[25] observed a strong absorption in KI: CN at 81.5cm^{-1} which they explained as a local mode in the gap, and broad absorptions between 35 and 70cm^{-1}, interpreted as resonant modes in the acoustic continuum.

The spectrum was similar to that obtained in KI: Cl[26]. The absence of a second gap mode might be explained through rapid reorientational motion, even though the primary motion of the molecule at low temperatures is librational they can still reorient very rapidly, of the CN^- ion about its two axes of inertia which causes it to behave like an ion of spherical symmetry. This model leaves the 68 cm^{-1} mode observed in this work unexplained.

The center of mass of the ion may not coincide with the centre of the large highly polarizable I^- cavity, as recently suggested by Pohl [27,28]. The close spacing of the difference satellite indicates that the potential to which the molecule is subjected in KI is different from that in KCl. The translational or librational motion around this off-center position may be responsible for some of the high-energy satellites. The only conclusion that can be drawn at this stage is that the existence of some oscillatory motion seems quite possible in the KI lattice and this may explain the persistence of the Q-branch at high temperatures. The beginning of this may already be observed in KBr and RbCl.

The CN^- spectrum in NaCl and NaBr is quite different from that observed for the other host lattices. The absence of P and R branches, the extreme narrowness of the vibrational transition even at temperatures as high as 80^0K, and the fact that the half- width of the band does not follow a $T^{\frac{1}{2}}$ law indicates that the barrier to rotation in NaCl and NaBr is extremely high and almost certainly greater than $100cm^{-1}$.

Unfortunately, an accurate estimate of the barrier height cannot be given because a librational satellite for the CN^- has not been observed in these two host lattices. From experimental sensitivity we estimate that any librational transition must be at least 50 to 100 times weaker than the fundamental at low temperatures. This indicates that the CN^- sits in a very harmonic potential well so that the Q-branch always dominates the absorption. The origin of the T^2 dependence of the half width is unknown but it is interesting to note that it is similar to that observed in the near infrared spectrum of U centers.

Under uniaxial stress the potential wells in the direction of the stress become deeper and the wells perpendicular to the stress become shallower. A repopulation of the molecules into the deeper wells may occur by the two processes mentioned above. Since the uniaxial stress experiments in this study we carried out below 4^0K it is sufficient to raise or lower the wells by only a few degrees Kelvin to observe an alignment.

The maximum dichroism was observed for [100] stress, a smaller dichroism for [110] stress with the light propagating parallel to [110].

Hence, we conclude that the equilibrium orientations for the dipoles are the <100> directions. The T^{-1} dependence shows the dichroism indeed arises through a molecular reorientation under the influence of the external stress. For small stresses the alignment should vary linearly with the applied stress. Departures from this law are observed for stresses smaller than 1 to 1.5kg/mm^2. From this one deduces a zero- stress splitting of ~ 0.6cm^{-1}. It may be attributed to a residual internal stress or to the fact that the ground state of the CN^- is split by tunneling, 1.4 and 2.4cm^{-1} as predicted by Devonshire. In his work on the R-center Silsbee[29] found similar deviations from a Langevin curve from which he deduced a zero-stress splitting of ~1.0kgmm^{-2}. Sussmann[30] used 3kg/mm^2 to explain the deviations observed by Kazing[31] for the 0_2^- center in KCl.

With <100> equilibrium orientations no optical dichroism should be observed for [111] stress. Hence the non vanishing dichroism is surprising. It cannot be caused entirely by inaccuracy in such a procedure, which is at most 5^0. It is conceivable that the residual internal stresses may tilt the direction of the applied stress for some of the centers so that the stress and the polarized light are no longer perpendicular to each other. There may also be a small probability for the molecules to orient along the <111> directions. In that case we would expect for higher potential barriers, smaller tunnel splitting, the dichroism for [111] stress to be smaller or even to disappear. Finally, and most importantly, the stress dependence of the energy levels is unknown. For these reasons we have not attempted to make a quantitative fit to the data and merely conclude that the alignment is of the Langevin type and the equilibrium orientations of the dipoles

are the <100> directions. For [111] stress the light was propagated both in [111] and [110] directions. Within experimental error the magnitude of the effect was the same. An nonvanishing dichroism was also found for [110] stress and light propagating in [010], with an alignment of 0.35 for a stress of ~ 5kg mm^{-2}.

The alignment observed in KBr, KI and RbCl host lattices is similar to that observed in KCl but smaller in magnitude. In all these host lattices the alignment proceeds with a time constant which is much faster than the time constant of our detection system (~2 sec.). Since in the potassium series the barrier height for the CN^- is low, both the classical thermal activation process discussed above and the tunneling process have a relaxation time which is shorter than our experimental time constant and it is not possible to decide which process is responsible for the observed alignment. In RbCl the classical process, owing to the high barrier, has a negligible probability at 1.36^0K. This implies that the alignment observed in this host lattice is through a tunneling process. From similar arguments the complete lack of alignment observed in NaCl and NaBr between 1.36 and 4.2^0K over time periods as long as 10^{-3} sec. implies that the tunneling frequency must be smaller than 10^{-3} sec^{-1} and the barrier to rotation must be greater than 100 cm^{-1}, assuming a librational frequency of 10^{12} sec^{-1}.

Recently Sack and Moriarty[28] measured the dielectric constant of KCl : CN, KBr: CN, KI: CN and NaCl: CN down to about 2.5^0K and in the frequency range 1-100 Kc/sec. They found in the potassium series that the dipoles followed the field oscillations but in NaCl they observed no increase in the dielectric constant. Their results are in excellent agreement with the conclusion drawn from our optical

data. They found a dipole moment of ~ 0.3 Debye for the CN^- in the potassium salts. The small dipole moment accounts for the fact that electric fields of 80KV/cm cause a change of less than 5% in the CN^- infrared band at 2^0K. So far as the equilibrium orientations of the CN^- is concerned, Pauling's calculation is repeated with a more realistic potential function in three dimensions and with six potential minima along the <100> directions This will also provide us with quantitative values of the tunnel splitting.

The tunneling probability can be calculated by starting with the librational wave function and then treating the effect of the anharmonic terms in the potential function as a perturbation. For low potential barrier, as in the case for CN^- in many alkali halides, a second method may be used. This consists of starting with the free rotor states and then calculating the effect of a crystalline electric field on the (2J+1) fold degenerate j^{th} rotational state. This method has been discussed by Devonshire[32] who calculated the energy levels for a linear molecule in an octahedral site. This is the lowest order surface harmonic of octahedral symmetry. Such a potential is obtained by considering the electrostatic field due to an octahedron of charges and is often used to study the spitting of the energy levels of paramagnetic atoms in an octahedral field.

The potential function used by Devonshire is

$$\tilde{V}(\theta,\varphi)=\left(-\tilde{k}/8\right)\left(3-30Cos^2\theta+35Cos^4\theta+5Sin^4\theta\times Cos^4\theta\right).....(1.7)$$

Where $\tilde{k}$ is a constant. For $\tilde{k}$ positive $\tilde{V}$ has six minima equal to $-\tilde{k}$ at the points.

$\theta = 0$ or π; $\theta = \pi/2$, $\phi = 0, \pm \pi/2$ or π

which correspond to the six <100> directions in the crystal. The potential maxima lie along.

$\theta = Cos^{-1}\left(\pm 1/\sqrt{3}\right), \phi = \pm\pi/4$ or $\pm 3\pi/4$.

which are the eight <111> directions in the crystal. Two wells lying in adjacent <100> directions are separated by a potential barrier of $1.25\tilde{K}$ in the <100> directions.

Devonshire[32] has given the energy eigenvalues of the Schrodinger equation for the potential $\tilde{V}(\theta,\phi)$. For $\tilde{K}=0$ the solutions reduce to the free- rotor energy levels. For $\tilde{K}\neq 0$, the degeneracy of the rotational energy levels is partly removed. The energy levels for J = 0, 1, 2, 3 have been plotted in units of the rotational constant $\tilde{B}$ as a function of $\tilde{K}/\tilde{B}$ and are shown in the fig (1.17). For high positive value of barrier parameter, $\tilde{K}$, the A_{1g} (J=0) T_{1u} (J=1) and E_g (J=2) states have very nearly the same energy. In the high-barrier limit they present a six fold degenerate libration ground state as should be the case for the six minima potential considered. The T_{2g} (J=2) will represent the first excited lib. state.

Using the well known electric dipole selection rules[23] the value of the barrier parameter $\tilde{K}$ can be determined from the observed splitting of the libration sum satellite T_{1u} (J=1)$\rightarrow T_{2g}$(J=2). Note that all transitions occur simultaneously with a change $\Delta\upsilon$= +1 in vibrational quantum number of the C-N stretching vibration.

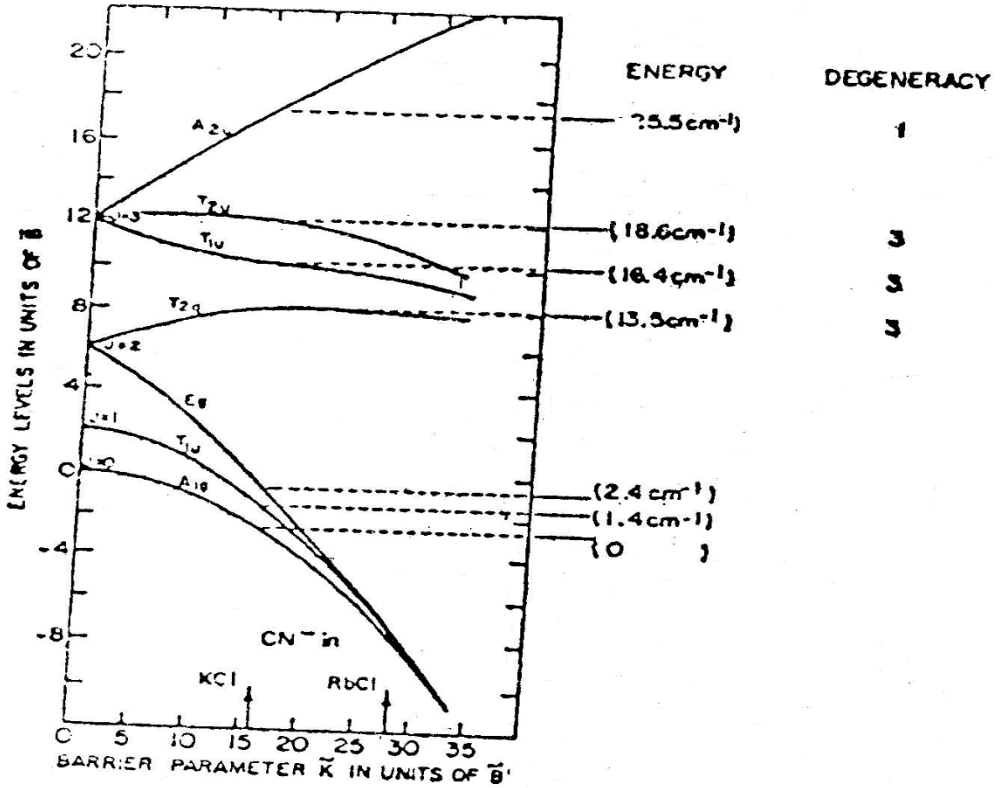

Fig. 1.17: The energy levels in units of $\tilde{B}$ as a function of the barrier parameter $\tilde{K}/\tilde{B}$ for a linear molecule in an octahedral site.

For a splitting of 12cm^{-1} it follows that $\tilde{K}=16\tilde{B}$=20cm^{-1}. From this a barrier height in <110> is determined to $\tilde{V}_0=1.25\tilde{K}$=25cm^{-1}. It is gratifying to find that the sophisticated Devonshire model yields a barrier height in very close agreement with the one determined from the simple two well Pauling potential, for which $\tilde{V}_0$=24cm^{-1} was found. In fig. (1.17) the level scheme for CN^- in the potassium halide is shown with the appropriate energies. Sum transitions from $A_{1g}^*(J=0)\rightarrow T_{1u}(J=3)$ and T_{2u}(J=3) with ΔJ=3 should be less likely. Transitions from E_g(J=2) to T_{1u} and T_{2u} (J=3) should be possible if E_g is thermally populated. These transitions may be partly responsible for the observed breadth of the sum satellite. However, note that T_{1u}(J=3) and T_{2u}(J=3) lie so close to the barrier in

contrast to $T_{2g}(J=2)$ that they are more appropriately called rotor states and hence would have a smaller probability of mixing with the librational $E_g(J=2)$ states[33]. The optical transitions giving rise to the strong central line in the absorption spectrum at low temperature are $A_{1g}(J=0) \rightarrow T_{1u}(J=1)$ and the inverse, $T_{1u}(J=1) \rightarrow A_{1g}(J=0)$. Note that these transitions are not, strictly speaking, Q-transitions. The Q transitions are partly forbidden.

The two transitions $T_{1u}(J=1) \leftrightarrow A_{1g}(J=0)$ different by $2.8cm^{-1}$ could not be resolved except in KI (at $2064.5cm^{-1}$) shown in fig. (1.7) despite accurate instrumental resolution ($0.6cm^{-1}$).

The width of the observed hand is, however, $2.5cm^{-1}$. The difference satellite arises above 10^0K because of thermal population of the T_{2g} (J=2) and of the $T_{1u}(J=3)$ and possibly the $T_{2u}(J=3)$ states. The selection rules predict a difference transition $T_{2g}(J=2) \rightarrow T_{1u}(J=1)$ at $12cm^{-1}$, plus transitions $T_{1u}(J=3) \rightarrow T_{2g}(J=2)$ at $2.9cm^{-1}$ and $T_{2u}(J=3) \rightarrow T_{2g}(J=2)$ at $5.1cm^{-1}$. What we observe is one broad band separated by less than the separation of the sum satellite.

Similarly, the librational frequency of $19cm^{-1}$ in RbCl yields $\tilde{K}=28$ $\tilde{B}=35cm^{-1}$. The T_{1u} and E_g levels are expected to lie 0.625 and $0.75cm^{-1}$, respectively above the A_{1g} state. This would predict a difference satellite $1.2cm^{-1}$ away which was again not resolved. However, the experimentally observed width of the central line in RbCl is about $1cm^{-1}$, i.e. much smaller than that observed in KCl and is qualitatively consistent with our supposition that the width arises from unresolved tunneling transitions.

1.5 Objective of The Book:

The IR measurements or CN^- in KCl, KBr, KI and RbCl have shown that at high temperatures the molecules can rotate freely in the lattice. At low temperatures the molecules perform librational motions with a frequency of 11 to 12 cm^{-1} in RbCl. In addition uniaxial stress measurements show that in these host lattices the CN^- can reorient down to the lowest temperature of our measurements (1.36^0K), the minima in the potential function being the <100> directions.

In NaCl and NaBr the CN^- is "locked-in" at low temperatures and the barrier hindering rotation is estimated to be greater than 100 cm^{-1}.

Finally, the energy levels of the CN^- in a six-well potential have been quantitatively considered for the potassium halides and RbCl in terms of the Devonshire model. This model can explain the gross features of the IR data but predicts tunneling transitions which were not observed in our optical measurements.

ISBN: 978-81-949998-9-8

Chapter 2

Thermal Conductivity and CN^- doped Specific Heat of Alkali Halide Crystals using Phonon Spectroscopy Technique.

2.1 Introduction:

Devonshire[32] model explains the gross features of the IR data but predicts tunneling transitions which were not observed in optical measurements. If this model is applicable and correct for the CN^- then the tunneling transitions in the IR data should be resolved and one can account for the fact that the rotational fine structure of the P and R branches at high temperatures resolved. These discrepancies can be satisfactorily explained by thermal conductivity of KCl, KBr and NaCl containing CN^- and the specific heat measurement of KCl: CN.

To answer the questions posed in the preceding chapter we have measured the thermal conductivity to study the phonon interactions in CN^- doped crystals. In contrast to optical spectroscopy, phonon spectroscopy via thermal conductivity is a broad band technique. Instead of a phonon monochromator one passes essentially a black body distribution of phonons down the crystal by means of a thermal gradient. The thermal conductivity is the transmission of this spectrum by the crystal integrated over all phonon frequencies. To unfold the phonon-scattering rates a method of curve- fitting is used that has been previously described and tested [34,35]. Limitations of the simple theory in the presence of strong normal processes have been recently discussed by Berman and Brock[36] and Thacher.

2.2 Data and Curve Fitting for KCl : CN:

The thermal conductivity of the system KCl: CN is shown in fig. (2.1). The striking features of the doped crystals are the great reduction in conductivity and

the distinct depressions in the curves at 0.6^0 and 7^0K. From this it follows that certain phonon frequencies interact very strongly with the CN^-. It is these resonance frequencies that we wish to correlate with infrared spectroscopic data. For a quantitative analysis of the scattering we use the Debye model for the thermal conductivity. Then the thermal conductivity K(T) is given by the following equation.

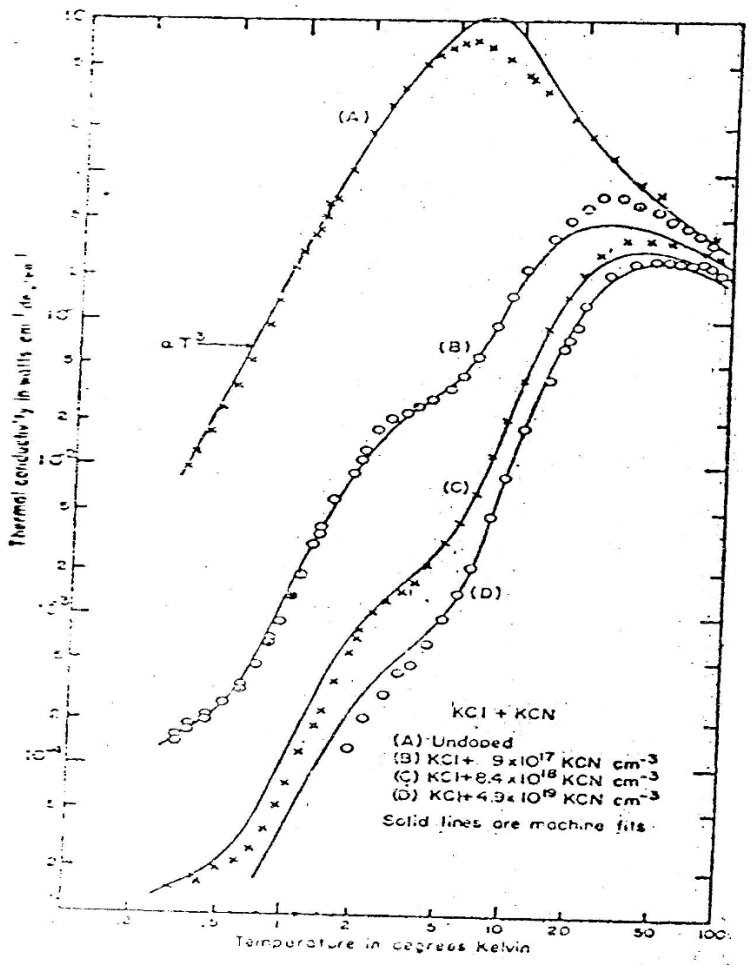

Fig. 2.1: Thermal conductivity of KCl: CN. CN^- concentrations are: (A) undoped, (B) 9 $\times 10^{17} cm^{-3}$ (C) $8.4 \times 10^{18} cm^{-3}$ (D) $4.9 \times 10^{19} cm^{-3}$. NCO^- concentrations are 1.3×10^{18} cm^{-3} Solid lines are machine fits.

$$K(T) = \frac{1}{2\pi^2 v} \int_0^{W_D} \Gamma(T, W) \frac{\hbar^2 W^4}{kT^2} \frac{e^{\hbar w / kT}}{\left(e^{\hbar w / kT} - 1\right)^2} dw \quad \text{.....(2.1)}$$

where υ is the sound velocity, W_D is the Debye cutoff frequency and Γ (T,W) is the combined relaxation time given by

$$\Gamma^{-1}(T,W)=\sum_j \Gamma_J^{-1}(T,W) \qquad \text{..... (2.2)}$$

In this equation $\Gamma_J^{-1}(T,W)$ is the relaxation rate of the j[th] scattering mechanism. The combined relaxation rate giving the best fit to the pure KCl data is:

$$\Gamma_P^{-1} = 4.9\times10^5 \text{ sec}^{-1} + 6.07\times10^{-44} \text{ sec}^3 W^4$$

$$+3.64\times10^{-18} \text{ sec deg}^{-1} \text{ Tw}^2 \text{ e}^{-40 \text{ K/T}} \text{..... (2.3)}$$

The individual scattering terms are boundary isotope, and umklapp, respectively and their origin is discussed in reference[37]. The average sound velocity used here is calculated from the Debye temperature θ, using the equation:

$$v=\theta^{h-1}\left(6\pi^2 n\right)^{\frac{1}{3}} = 2.5\times10^6 \text{ cm/sec..... (2.4)}$$

where *n* is the number of atoms per unit volume. The accuracy of the pure- crystal fit is more than adequate since in fitting the doped crystals one has to add a relaxation rate that completely dominates the pure- crystal rate except at high temperatures. The doped crystals were fit with the following relaxation rate that had previously been used to fit KCl: NO^-_2 data:

$$\Gamma^{-1} = \Gamma_P^{-1} + N\left[\frac{D_1 W_1^2 W^2}{\left(W_1^2 - W^2\right)^2 + \Gamma_1^2 W_1^2} + \frac{D_2 W_2^2 W^2}{\left(W_2^2 - W^2\right) + \Gamma_2^2 W_2^2}\right] \text{.....(2.5)}$$

The scattering rate for each depression had to have a resonance from falling off rapidly on both sides of the resonance frequency. The expression used satisfies these requirements and in addition has a very plausible from analogous to the scattering rate of phonons by atomic states. A similar case has been treated by

Griffin and Carruthers[38]. They calculated the scattering rate by donor electrons in germinium and obtained an expression similar to that used here except for the frequency dependence of the numerator which comes from a detailed knowledge of the electron-phonon interaction. Calculations of the scattering of phonon by molecules have been made by Wagner using both perturbation theory[39] and Green's function techniques[40]. His scattering rate were of a resonance type note greatly different from that used here. However, sufficient details of the phonon molecule interaction were not included and so comparison with experiment was not possible. It was recently suggested by Sussmann[41] that tunneling included by single phonon could be responsible for the phonon scattering by molecules. His calculation was based on scattering between states split by the residual internal strain and he found a phonon- relaxation rate proportional to the phonon frequency in contrast to our results.

At present it appears that there is no firm theoretical basis for the use of equation (2.5). We therefore, merely state that it fits that data well and proceed to use it in determining the resonance frequencies.

The constants $D_1 = 1.16\times10^{-10}$ cm^3 sec^{-1}, $D_2 = 7.5\times10^{-10}$ cm^3 sec^{-1}, $\Gamma_1 = 0$, $\Gamma_2 = 0$, $W_1 = 3\times10^{11}$sec^{-1} $\left(\tilde{\upsilon}_1 = 1.6cm^{-1}\right)$ and $W_2 = 3.54\times10^{12}$ sec-1 $\left(\tilde{\upsilon}_2 = 18cm^{-1}\right)$ were chosen to give the best fit to the data for the sample B. N was the optically determined CN^- concentration in this crystal. The damping terms Γ_1 and Γ_2 could be as large as $0.4W_1$ and $0.4W_2$ respectively without making the fit to the data. This is because the damping affects negligibly. For the samples (C) and (D) the effective values of N were determined to give good agreement between the machine fit and the data in the temperature range 5^0 to 20^0K. The scaling of the strength of the phonon scattering with CN^- concentration is demonstrated by the effective values of N for curve (C) and (D) 11.6×10^{18}cm^{-3} and 3.7×10^{-9}cm^{-3} respectively, which agree within the experimental error with the optically determined CN^-

concentration, $8.4\times10^{18}cm^{-3}$ and 4.9×10^{19} cm^{-3} respectively. The phonon scattering does not scale with NCO^- concentration which varies by only a factor of 3 between samples (B) and (D). From this together with the fact that the infrared spectra of NCO^- consist of very narrow lines we conclude that NCO^- does not scatter phonons.

2.3 Origin Of The Resonance Frequencies In KCl : CN:

A very plausible origin for the phonon resonance frequencies W_1 and W_2 can be seen from the energy- level diagram of CN^- in KCl, Fig. (2.2)

The resonance energy $\hbar w_1$ ($1.6cm^{-1}$) is very nearly equal to the tunneling splitting. This suggests that the low-temperature depression in the thermal-conductivity curves is caused by a resonance phonon absorption in which the CN^- is excited from the ground state, A_{1g}, to one or both of the next two levels, namely T_{1u}($1.4cm^{-1}$) or E_g ($2.4cm^{-1}$), subsequent de-excitation of the molecule would result in the emission of a phonon of the same energy but in a random direction. Thus the over-all process would add to the thermal resistance. Such a strong phonon interaction would cause appreciable broadening of levels T_{1u} and E_g and could explain why the tunneling splitting was not resolved in the infrared spectra. It is not possible to say that $A_{1g}\rightarrow T_{1u}$ is favoured over $A_{1g}\rightarrow E_g$ or vice versa. Since the energy levels are not that accurately known and in addition the thermal conductivity data can not be fit that precisely.

The $T_{1u}\rightarrow E_g$ transition, however, cannot have an appreciable effect on the thermal conductivity since in order to populate T_{1u}, one has to go to temperatures so high that the dominant phonons have energies considerably larger than the separation of T_{1u} and E_g. The dominant phonons in carrying the heat current at low temperatures have the energy $hw_M \approx 4kT$. Where w_M is the frequency for which the integrand, apart from Γ, in the thermal- conductivity integral is a maximum.

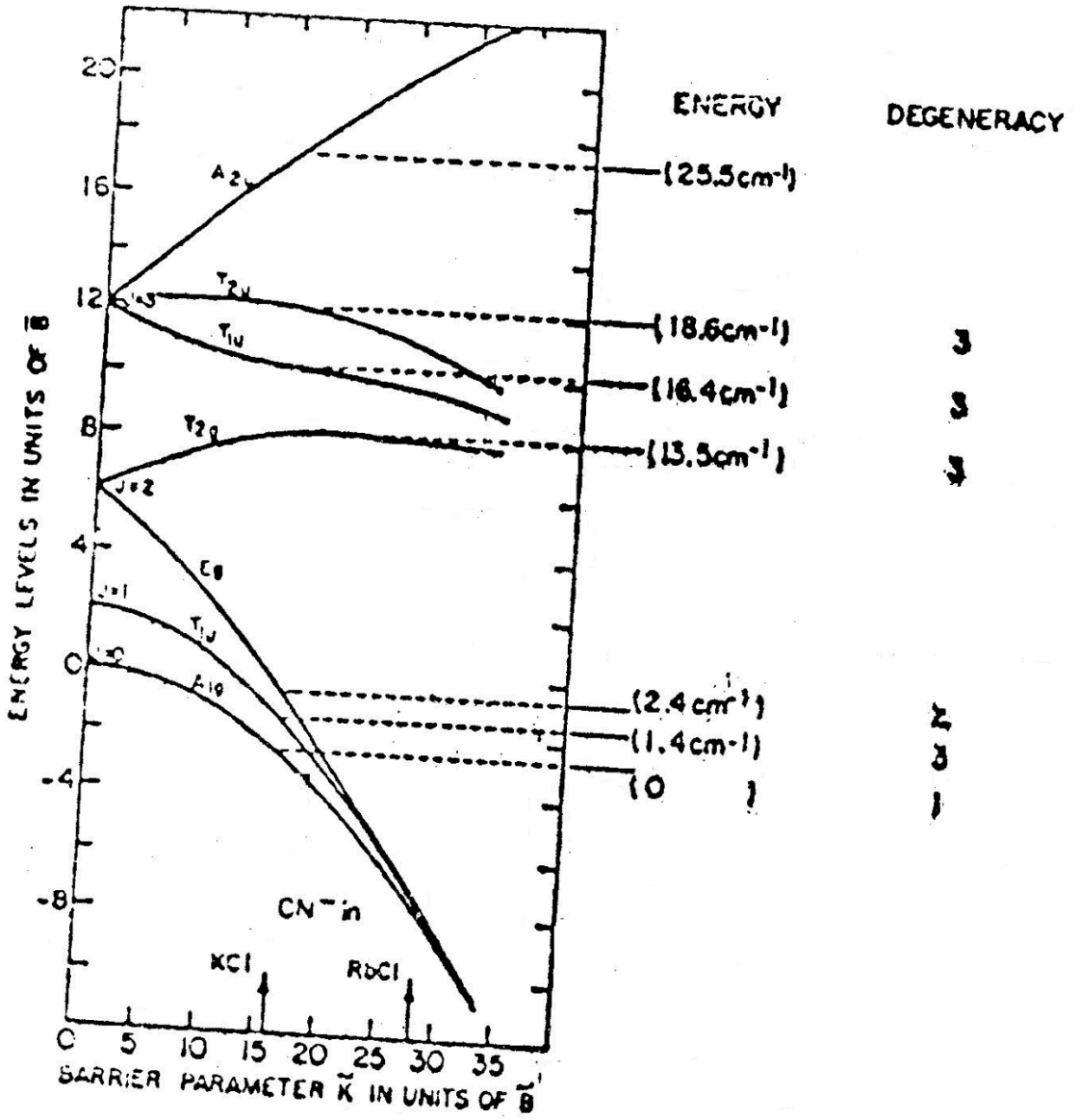

Fig. 2.2. The energy levels in units of $\tilde{B}$ as a fuction of the barrier parameter $\tilde{k}/\tilde{B}$ for a linear molecule in an octahedral site.

The second dip in the thermal conductivity requires a phonon resonance energy of $\tilde{\upsilon}_2$ =18cm^{-1} which is about equal to that positions of the T_{1u} (16.4cm^{-1}) and T_{2u} (18.6cm^{-1}) levels.

We conclude that there is a strong phonon coupling between these states and the tunneling states. Transitions to the librational level T_{2g}(13.5cm^{-1}) are not observed in the thermal conductivity.

This is in agreement with the low-temperature infrared spectra which indicate that the librational level is not greatly broadened. Furthermore, it appears generally true that librational levels do not scatter phonons strongly since NCO^- in KCl which does not affect the thermal conductivity has librational levels spaced at about $4cm^{-1}$.

No scattering by transitions to higher energy levels beginning at $25.5cm^{-1}$ is reflected in the thermal conductivity. There are several reasons for this. Some transitions will be eliminated by selection rules on the matrix elements. Secondly, there may be a mismatch between the energies of the allowed transitions and the energies of the dominant phonons available at a particular temperature. This combined with population considerations for the CN^- levels could rule out the possibility of seeing dips at higher temperatures. Finally, the umklap scattering rate increases exponentially with temperature and eventually dominates all other scattering mechanisms.

We should note that the T_{1u} ($16.4cm^{-1}$ and T2u ($18.6cm^{-1}$) levels, which we believe to be responsible for the depression in the thermal conductivity at 6^0K, lie just about at the top of the potential barrier ($19cm^{-1}$) above A_{1g}) and hence are the first rotational states of the molecule. Phonon-induced transitions between higher rotational states although not observed in the thermal conductivity, would account for the missing fine structure in the high temperature infrared spectra.

2.4 Thermal Conductivity of KBr: CN, KI: CN AND NaCl: CN

Fig. (2.3) shows that the phonon scattering by CN in KBr is very nearly the same as in KCl. The only difference is that the 6^0K resonance in KBr: CN is considerably broader. Here again the positions of the resonance can be explained in the same way as in the case of KCl: CN since the infrared spectra of KBr: CN and KCl : CN are virtually the same.

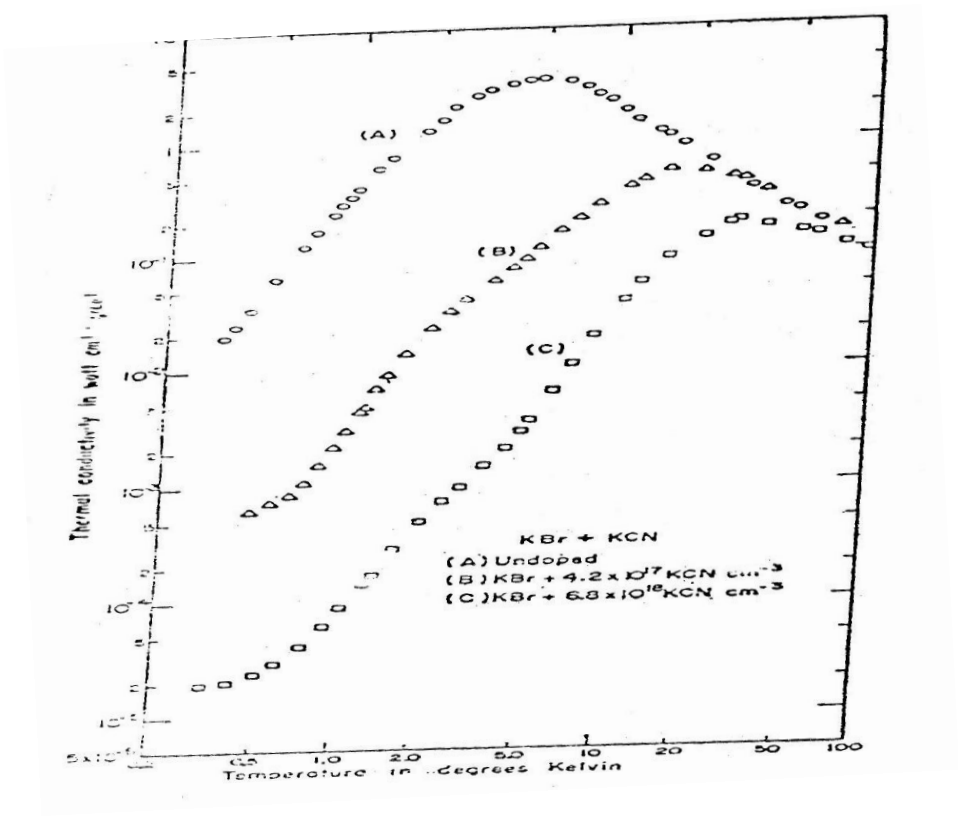

Temperature in degrees kelvin

Fig. 2.3 Thermal conductivity of KBr: CN. CN^- concentrations are: (A) undoped, (B) $-4.2\times10^{17}cm^{-3}$ (C) $-6.8\times10^{18}cm^{-3}$, NCO^- concentrations are B-3×10^{18} cm^{-3} and C-$7\times10^{18}cm^{-3}$.

The thermal conductivity of one KI crystal containing 5×1019 CN^- cm^{-3} was measured between 0.3^0 and 1.5^0K. The data points were almost identical to those in the lower portion of the curve C in Fig. (2.3).

Since the CN^- concentration in the KI crystal was about 5 times that in the sample (C) we conclude that the scattering is weaker in KI but otherwise the same for small w(1.6×10^{11}–8×10^{11} rad. sec^{-1}).

The weaker coupling to the phonons as reflected in the thermal conductivity is consistent with the optical data for CN^- in KI where there are the first indications of the resolution of the tunneling splitting.

In the previous three systems two resonances in the phonon scattering can be explained with the energy level diagram based on spectroscopic data.

One of the phonon resonance energies matches the tunneling splitting of the CN^-. The other matches the energy difference between the ground state and rotational states lying at the top of the potential well.

To test the generality of this model CN^- in NaCl was studied. Here the infrared spectra show that the CN^- is frozen in there is no tunneling splitting and the rotational states lie at least $100cm^{-1}$ above the ground state.

We would expect, therefore, no effect on the thermal conductivity except perhaps at high temperatures. Fig. (2.4) shows the NaCl: CN thermal conductivity results. Indeed, at low temperatures the CN^- has no effect.

The depression at 40^0K may be caused by scattering of the CN^- both as a molecule and as a point defect. Similar high temperature depressions have been observed in the thermal conductivity of crystals containing about the same concentration of monatomic defects[37].

Assuming, however, that the scattering is caused by rotational states of the CN^- lying at the top of the potential barrier. We estimate the barrier height to be $140cm^{-1}$ from the position of the dip in the thermal conductivity.

This is in agreement with infrared data discussed proviously which place the barrier about $100cm^{-1}$.

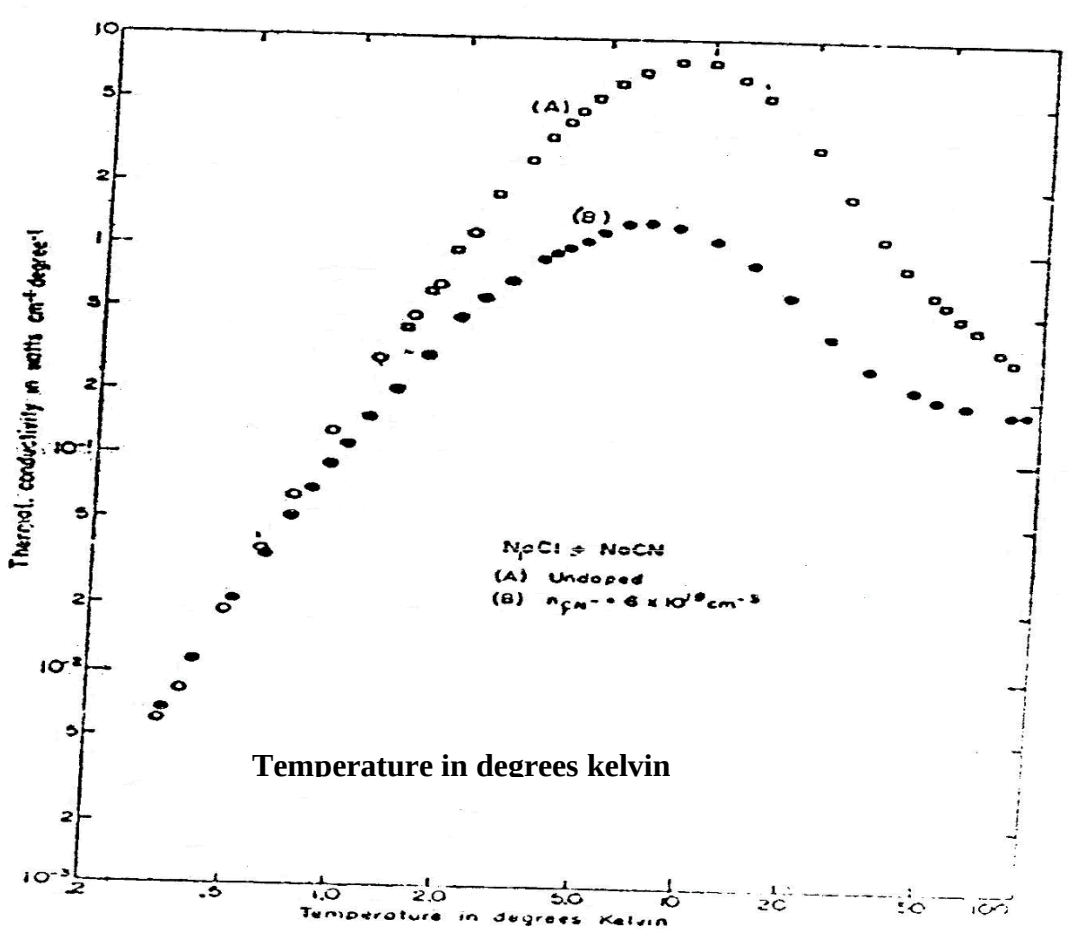

Fig. 2.4: Thermal conductivity of NaCl: CN (A) undoped (B) has 6×10^{19} CN^{-} cm^{-3} and 5×10^{17} NCO cm^{-3}.

2.5 Specific Heat of KCl^{-} : CN

Direct evidence for the existence of the tunneling splitting can be obtained with specific heat measurements. The tunneling states should produce a Schottky type anomaly similar to that found in paramagnetic salts having a ground state which is split by the crystalline field[42].

Ignoring for the moment all levels but the tunneling levels the specific heat may be written as:

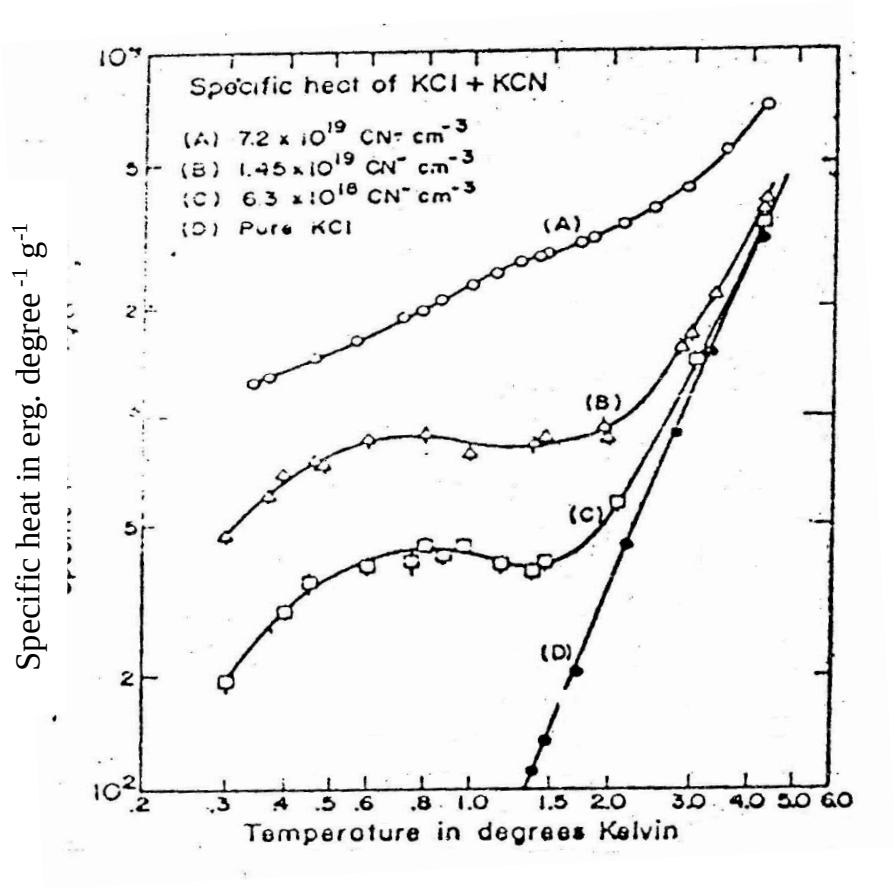

Fig. 2.5: Specific heat Cv of KCl^{-} : CN.

$$C_t = N\frac{\partial}{\partial T}\left(\frac{g_1\Delta_1 e^{-\Delta_1/kT} + g_2\Delta_2 e^{-\Delta_2/kT}}{g_0 + g_1 e^{-\Delta_1/kT} + g_2 e^{-\Delta_2/kT}}\right) \text{.....(2.6)}$$

Where, 0, 1 and 2 refer to the A_{1g}, T_{1u} and Eg levels respectively, Δ_i is the energy of the j^{th} level above the ground state, A_{1g},g_i is the degeneracy of the j^{th} level, and N is the number of molecules.

From this expression the entropy may be calculated and particularly the change in entropy in going from temperature in which all of the molecules are in the ground state to one in which there is an equal probability for the molecule to be in any one of the 6 states. From statistical mechanics this change in entropy is $\Delta s = k \ln 6$ per molecule and is independent of how the levels are spaced.

The measured specific heat of KCl: CN is shown in the fig. (2.5). The graph shows dramatically the size of the anomaly relative to the size of the lattice specific heat, curve D, but in order to analyse the anomaly the lattice specific heat must be subtracted fig. (2.6). The theoratical curve (1), calculated from equation (2.6) using the energies and degeneracies from fig. (2.2), is the expected Schottky specific heat for same (B). Curves (B) and (C) exhibit the same shape below 1.5^0K indicating that the level spacing is in reasonable agreement with the predicted but both curves are broader than calculated. We attribute this broadening to the residual strain in the crystal that was previously discussed.

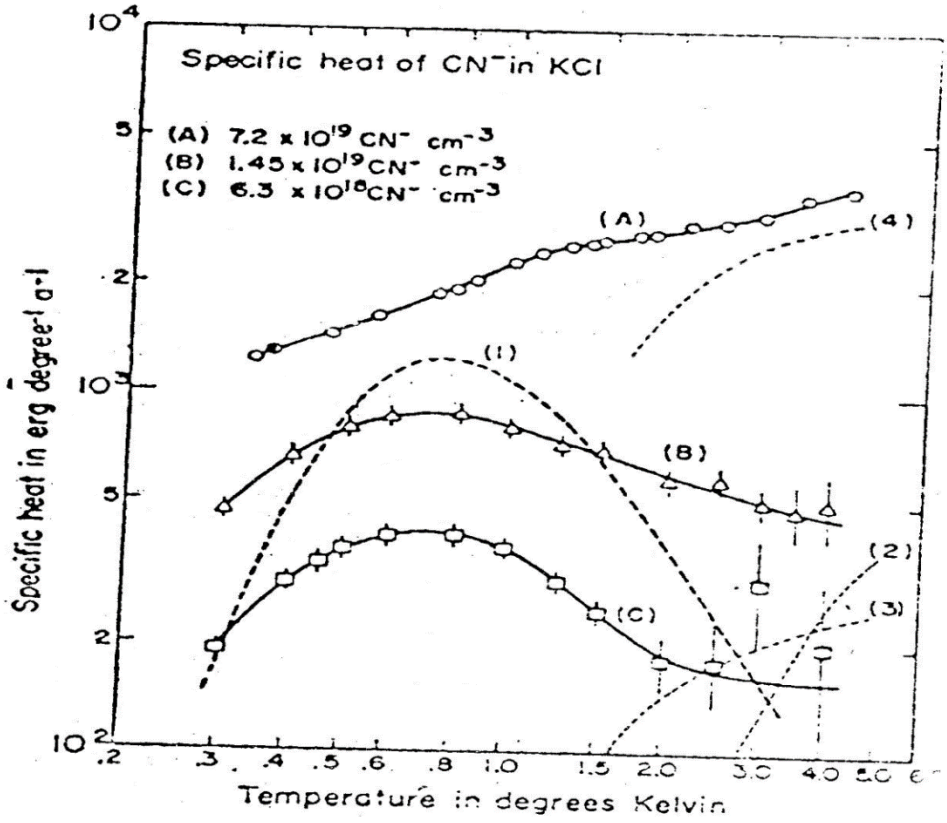

Fig. 2.6: Curve A, B, C are the specific heat of KCl: CN with KCl lattice specific heat subtracted.

For a quantitative comparison between theory and experiment the change in entropy ΔS was determined by graphical integration of the measured Cv/T curves between 0.3^0 and 4.2^0K.

$$\Delta S_B = N_B \, k \, In \, (6.3+0.6)$$

$$\Delta S_c = N_C k \, In \, (5.6 \pm 0.6) \ldots\ldots\ldots\ldots\ldots\ldots \quad (2.7)$$

This demonstrates not only that the specific heat anomaly scales with the CN^- concentration but also that the tunnelling levels in fact consist of a total of 6 states as expected in the case of six <100> equilibrium orientations. Curve (A), N = $7.2\times10^{19}cm^{-1}$, does not show the expected maximum in the specific at 0.7^0K. Its shape is somewhat similar to the specific heat measured on KCl: OH[43]. In our case, however, it is not possible to explain this as a dipole- dipole interaction leading to antiferroelectric ordering of the CN^- dipoles[44], with the smaller CN^- dipole moment and for this concentration the critical temperature T_C would be about 0.7^0K for a uniform distribution of the ions[45]. Unless the CN^- ions were nonrandom in crystal (A) we must assume that some other defects were producing a change in the energy levels of the CN^- ions. It should be noted that in this sample, compared to the samples of the IR and the thermal conductivity studies, the CN^- concentration was 10 times higher, $N_{NC0}= 2.5\times10^{19}cm^{-3}$. The librational energy levels of NCO^- ions and the higher states of the CN^- ion, fig. (2.2), certainly account for the rise in specific heat above 2^0K observed in all three samples, as indicated in fig. (2.6).

2.6 Influence of An Electric Field on The Thermal Conductivity:

An electric field should change the energy levels of the CN^- ion. Thus, effect turned out to be too small to be detected in the infrared. There is, however, a large effect on the thermal conductivity as shown in fig. (2.7). Therefore, the change in thermal resistivity on applying an electric field divided by the zero- field resistivity is plotted versus temperature. The curves are similar for KCl and KBr except that in KBr the curves are shifted to lower temperatures.

In order to understand this effect let us first assume that the electric field increases the ground state splitting of $1.6cm^{-1}$ which was expected from the thermal conductivity data as shown in fig. (2.1 and 2.8). We computed the conductivity for a splitting of $1.9cm^{-1}$ and found a change quite similar to the effect measured for KCl. Furthermore, assuming that this additional splitting ($0.3\ cm^{-1}$) is simply $\Delta = 2\mu CN^{-} \times E$. We determined for E = 30 kV/cm, $\mu\ CN^{-} \sim 0.3D$, in agreement with the accepted value.

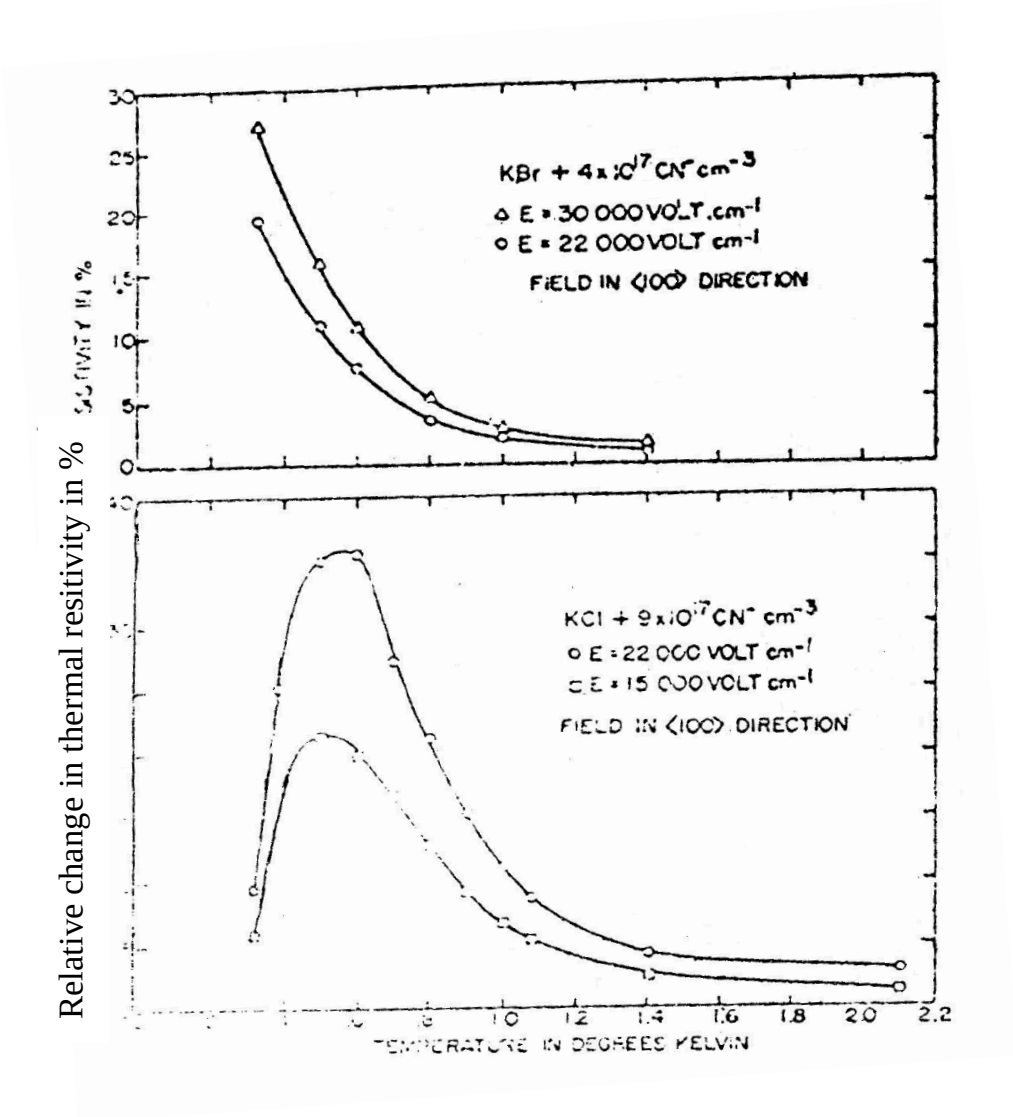

Fig.2.7: Relative change in thermal resistivity on applying an electric field E.

2.7 Discussion:

From fig. (2.4) we see that at low temperatures the CN^- has no effect. The depression at 40^0K may be caused by scattering of the CN^- both as a molecule and as a point defect. Similar high temperature depressions have been observed in the thermal conductivity of crystals constaining about the same concentration of nonatomic defects. Assuming that the scattering is caused by rotational states of the CN^- lying at the top of the potential barrier, we calculate the barrier height to be 140 cm^{-1} from the position of the dip in the thermal conductivity, which is in agreement with the I.R. data. A comparison of the KCl and KBr data shows that such sample picture is inadequate. Instead one must calculate the field dependence of the energy levels fig. (2.2) and it is conceivable that this would be different for the two host lattices. It appears that experiments of this kind can provide a better understanding of the lowest energy states of the molecules in solids.

Fig. (2.5) gives the measured specific heat of KCl: CN. The graph shows dramatically the size of the anomaly relative to the size of the lattice specific heat, curve D. In order to analyse the anomaly the lattice specific heat must be subtracted, fig. (2.6). The theoretical curve 1, calculated from equation (2.6) using the energies and degeneracies from equation (2.2), is the expected Schottky specific heat for the sample (B). Curves (B) & (C) exhibit the same shape below 1.5^0K indicating that the level spacing is in reasonable agreement with the prediction but both curves are broader than the calculated curves. The broadening is attributed to the residual strain in the crystal.

ISBN: 978-81-949998-9-8

Chapter 3

Shift of the Intramolecular Vibrational Line of OH- Impurity in Alkali Halide Crystals

3.1 Introduction:

Recently much more interests have been devoted to study the rotational degrees of freedom of molecules in solids. Experiments on the matrix properties of hydroxylation alkali halide crystals have presented several interesting features. The tunneling splitting, para electric resonance and the isotope effect of the librational frequencies have also been well understood in terms of Different theoretical models. Low temperature specific heat measurements have shown the existence of low-lying tunneling levels. Spectroscopic studies show the presence of librational lines. These librational lines are observed as sum satellites to the intramolecular vibrational absorption. The quantitative interpretation of these librational and tunneling levels has successfully been done in terms of Devonshire model. The band center is observed at different positions in the different crystal systems.

In the present chapter, we try to explain the shift of the intermolecular vibrational absorption of the impurity in different alkali halide crystals on Buckingham's theory. This theory can very well account for the observed shift of the band center of the CN^- impurity in alkali matrices, provided proper lattice distortion around the impurity is suitably considered. The amount of the lattice distortion needed to explain the observed shift agrees well with that obtained on the basis of Brauer's method of calculating lattice distortion.

3.2 Principle:

When a polyatomic impurity molecule is substituted in a crystal matrix, the molecular interactions between the impurity and the host crystal matrix ions

modify the stretching or bending vibrational spectra of the impurity in a number of ways as follows:

a. The frequency of the normal vibrational modes of the substituted impurity molecule may be shifted to higher or lower values.
b. The intensities of the bands may change by factors of ten or even more.
c. The half width of the lines may be greatly increased and
d. The combination bands involving simultaneous transitions in the impurity molecule and one or more of its neighbours may be induced.

A study of these spectral features can yield much information about the intermolecular as well as the intramolecular forces. In this chapter the study of the shift of the stretching frequency of OH^- ions trapped in alkali halid crystal matrices has been predicted.

Buckingham[46] has evaluated the effects of the solute solvent interaction on the vibrational spectrum of a dissolved molecule in a solvent matrix. The essential assumption of this theory is that of the interaction energy *U* between the impurity molecule and the near neighbours can be expanded, as a power series in the normal coordinates η of the impurity molecule. The normal co-ordinate η is defined as:

$$\eta = (r - r_e)/\, r_e \text{.....(3.1)}$$

where r is the intermolecular separation of the impurity molecule and r_e is its equilibrium value.

The total Hamiltonian H_s for the problem is given by

$$H_s = H_0 + \frac{\hbar c w_e}{4B_e}(A\,\eta^3 + B\eta^4 + \text{.....} + U) \text{.....(3.2)}$$

$$\text{Where } H_0 = \frac{1}{2}\overset{*}{M} r_e^2 n^2 + \left(\frac{hcw_e}{4B_e}\right)n^2 \quad \text{.....(3.3)}$$

is the unperturbed Hamiltonian. The second and the third terms on the RHS of the equation (3.2) are the anharmonic and the interaction energy terms respectively. In Buckingham theory[46] these terms are treated as perturbation to the unperturbed harmonic oscillator Hamiltoniam, H_0. By applying the 1st and second order perturbation theory, the Eigen values of the Hamiltonian H_s for the nth state are evaluated as:

$$W_{s_n} = W_n\left(n+\frac{1}{2}\right)\frac{B_e}{W_e}\left(U''-3\frac{A}{W_e}U'\right) \quad \text{.....(3.4)}$$

$$\text{Where } W_n = \left(h+\frac{1}{2}\right)(hcW_e)\left[1+\frac{3}{2}\left(h+\frac{1}{2}\right)\frac{B_e}{W_e}\left\{\frac{B}{W_e}-\frac{5}{4}\left(\frac{A}{W_e}\right)^2\right\}\right] \quad \text{.....(3.5)}$$

The solvent shift for an absorption line appearing because of a transition from mth to nth state can now be worked out and written in a complete form as follows:

$$(\Delta W)_m \rightarrow n = \{(W_{s_n} - W_n) - (W_{s_m} - W_m)\}/\text{hc}$$

$$= (n-m)\frac{B_e}{bcW_e}\left(U''-\frac{3A}{W_e}U'\right) \quad \text{.....(3.6)}$$

Thus the shift of the fundamental ($0\rightarrow$) band -center is given by

$$(\Delta W)_0 \rightarrow 1 = \frac{B_e}{hcw_e}\left(U''-3\frac{A}{W_e}U'\right) \quad \text{..... (3.7)}$$

In the above equation, B_e is the rotational constant, W_e is the harmonic stretching frequency and A & B are the anharmonicity constant for the free molecule. U'

and U" are the first and second derivatives respectively, of the interaction energy U with respect to the normal co-ordinate η of the impurity molecule.[84-89]

In the present case of OH^- ions trapped in the alkali halide matrices, *U* may be written as

$$U = -\frac{6e^2}{R} - \frac{6\alpha_H \mu_s^2}{R^6} - \frac{6\alpha_H \theta_s^2}{R^8} + 6b \quad \exp\left(\frac{r_+ + r_- - R}{\rho}\right) \text{.....(3.8)}$$

Here the first term is the charge- charge interaction term and does not contribute to the shift of the band center.[90-91] The second and 3rd terms are the dipole-induced-dipole and the quadrupole- induced- quadrupole interaction terms respectively. These are the long range interaction terms and give a red shift to the frequency of the band center as follows:

$$(\Delta W)_{\substack{\mu-\alpha\mu \\ +\theta-\alpha\theta}} = -\frac{6B_e}{hcw_e} 2r_e^2 \alpha_H \left[\left(\frac{d_{\mu_s}}{dr}\right)^2 \frac{1}{R^6} + \left(\frac{d\theta_s}{dr}\right)^2 \frac{1}{R^8}\right] \text{.....(3.9)}$$

Where R is the distance between the molecular impurity and one of the nearest neighbours, μ_s and θ_s are electric dipole and quadrupole moments respectively of the impurity molecule and α_H is the polarizability of the nearest neighbour host-matrix ions.[92-95] The 4th term of the right hand side of equation (3.8) is the repulsive interaction term.

For this interaction we have taken the Born- Mayer- Huggins form of the potential. This gives a blue shift to the band centre, which may be expressed as,

$$(\Delta W)_{rep} = \left[A + \left(x^2 + 2x\right)/\rho^2 B - \frac{x}{p} C\right] \text{exp. (x).....(3.10)}$$

Where $x = (r_+ + r_- - R)/\rho$ .....(3.11)

and

$$A = \frac{6B_e}{hcw_e}\left[\frac{\partial^2 b}{\partial \eta^2} - 3\frac{A}{W_e}\frac{\partial b}{\partial \eta}\right]$$

$$B = \frac{6B_e}{hcw_e}\left[b\left(\frac{dp}{dn}\right)^2\right]$$

and

$$C = \frac{6B_e}{hcw_e}\left[2\frac{\partial b}{\partial \eta}\frac{\partial p}{\partial n} + b\left(\frac{\partial^2 p}{\partial n^2} - \frac{3A\partial p}{W_e \partial n}\right)\right] \text{.....(3.12)}$$

In these equations, b and ρ are the potential parameters of the Born- Mayer-Huggins generalized potential, b is a constant for the entire family of alkali halide crystals, whereas ρ changes from one type of interacting ion perpendicular to the other.

It can be seen that the parameter X depends on the nature of the matrix as well as that of the impurity. On the other hand, the parameter A, B and C depends only on the rate of change of the potential parameters with the vibrational state of the impurity.

3.3 Lattice Distortion Around the Oh^- Impurity In Alkali Halide Crystals:

A precise knowledge of lattice distortion around the point defects in solid crystals is of the first order importance in understanding the various properties connected with such defect systems.

These properties include the calculation of self energy of the defects, interaction between the defects the X-ray diffraction effect and the quadrupolar broadening of the NMR lines. There are two different lines of theoretical approach for calculating the lattice distortion around the substituted point defects.

The first line of approach is based on the isotropic elasticity theory. The second line of approach is based on the discrete nature of the lattice.

We have adopted the Brauer's method[47] of calculation which is based on the first type of approach.

The second line of approach has been used by Kauzaki and has been further developed by Hardy[49] and by Caldwell and Klein[50].

The method of Hardy and Caldwell and Klein are equivalent to each other. We have adopted the method of Caldwell and Klein for calculating the lattice distortion in our case.

3.3.1 Brauer's Method:

This method assumes that isotropic displacement of the near neighbour around the impurity. The displacement of the neighbouring ions is assumed to obey the inverse square law

$$u_{1mn} = \frac{u_0}{1^2 + m^2 + n^2} \quad \text{..... (3.13)}$$

Where u_0 is the displacement of the nearest neighbour ions and u_{1mn} is that of the ion at (1, m, n) lattice site.

The displacement $u = R_0$, (R_0= pure lattice constant) and the induced electronic dipole moment υ in the six nearest neighbours are treated as unknowns. These two unknowns are determined by solving the following two equations:

$$F_e + F_r = 0 \quad \text{.....(3.14)}$$

and

$$= - \frac{F_e \alpha}{e} \text{ .....(3.15)}$$

Here the first equation arises due to the equilibrium condition whereas second one comes from the definition of the induced electric dipole moment itself.

From the symmetry of the Fcc lattice it can be seen that the electrical force F_e and the repulsive force F_r are acting along the <100> directions. For the impurity doped alkali halide crystals, the electrical force F_e on (1, 0, 0) ion is given by

$$F_e = \frac{C^2}{R_0^2}\left[\frac{\left(\sqrt{2}+0.25\right)}{(1+\xi)^2} - \frac{4(1+\xi)}{\left[1+(1+\xi)^2\right]^{3/2}} - \frac{1}{(1+\xi)^2} + \frac{2.3713\upsilon}{(2+\xi)^3} + 1.577\xi\right] \text{ ..... (3.16)}$$

In this equation, the first, second and third terms on the right hand side represent the force on (1,0,0) ion due to the displacements of the five other nearest neighbours.

The Fourth term is due to the induced dipole moment υ in five ions. The last term gives the force due to the dipole moments associated with the elastic components of the ionic displacements.

The energy of the repulsive interaction between the (1,0,0) ion and its nearest neighbour is given by,

$$U_{rep} = \left[V_0(R_0+u_0) + V(R_0 - u_0 + u_{200}) + 4v\left\{R_0 + \left(\frac{1}{\sqrt{2}}u_{100}\right)^3 + \left(u_0 - \frac{1}{\sqrt{2}}u_{100}\right)^2\right\}^{\frac{1}{2}}\right] \text{(3.17)}$$

The function V are the Born- Mayer- Huggins generalised potential functions. The suffix refers to the potential energy between the impurity and the six nearest neighbour ions. Thus the repulsive Force F_r on the (1,0,0) ion may be obtained as,

$$F_r = -\frac{\partial U_{rep}}{\partial u_0} \text{.....(3.18)}$$

or,

$$F_r = \frac{b_s}{\rho_s} \exp \frac{r_s + r_+ - (1+\xi)R_0}{\rho_s}$$

$$+ 0.75\frac{b}{\rho}\exp\left(\frac{r_+ + r_-}{\rho}\right)\times\left[-\exp\left\{-\frac{R_0}{\rho}(1-0.75\xi)\right\}\right]$$

$$+\frac{4\exp\left\{-\frac{R_0}{\delta}\left[\left(1+\frac{1}{2\sqrt{2}}\xi\right)^2+\left(\xi-\frac{1}{\sqrt[2]{2}}\xi\right)^2\right]^{\frac{1}{2}}\right\}}{\left\{\left(1+\frac{1}{2\sqrt{2}}\xi\right)^2+\left(\xi-\frac{1}{\sqrt[2]{2}}\xi\right)^2\right\}^{\frac{1}{2}}}$$

The equilibrium positions of the nearest neighbour ions can now be determined from the equations (3.14) and (3.15) by using the graphical solution method.

3.3.2 Hardy's Method:

Hardy[49] considers a hypothetical super lattice of the impurity ions, which possesses the same structure as the host crystal lattice, and the unit cell much larger than that of the host crystal lattice.

Thus the ionic displacement is associated with the super- lattice periodicity and therefore, can be expanded in Fourier series. Then the Fourier transform of the displacement is obtained from the minimization condition of the increase in the energy of the system due to introduction of the impurity. The exact coulomb and the repulsive potentials are used in calculating the energy increase for the nearest neighbour ions.[86-88] For all other ions, it is approximated by a quadratic function of the displacements.

The final expression for the displacement, u_0, of the nearest neighbour ions is obtained by

$$u_0=\alpha_0 F_e \text{ ..... } (3.20)$$

Where α_0 is the constant depending upon the host- matrix only. The repulsive Force F_r, when the nearest neighbours are displaced by u_0, is given by:

$$F_r = \frac{\partial}{du_0}\left[V_s(R_0+u_0) - u_0 V'(R_0) - \frac{1}{2}u_0^2 V''(R_0)\right] \text{.....} (3.21)$$

The value of u_0 is obtained from the equation (3.20) and (3.21) by following an iterative procedure.

3.3.3 Caldwell And Klein's Method:

This method, although uses a different language, is equivalent to that of Hardy[49]. On substitution of the impurity, the force vector along the bond- length between the substituted site and the nearest neighbour sites changes. This change, in general, is given by

$$\Delta F^{jp}(L) = -\left[\left(\partial V_i / u^{jp}(L) - \left(\partial V_0 / \partial u^{jp}(L)\right)\right)\right] \text{.....} (3.22)$$

Where L denotes the unit cell, p denotes the type of the ion and j gives the certain co-ordinates x,y and z. R_0 is the old equilibrium position of the nearest neighbour ion and *u* is the displacement from the equilibrium position. The impurity is taken to be at the origin. The subscript 0 denotes the pure crystal bond and I denotes that of between the impurity and its nearest neighbours. The first term on the right hard side in equation (3.22) is evaluated at the new equilibrium position and the second one is evaluated at the old equilibrium position. The vector $\Delta F^{jp}(L)$ is localized and has A_{1g} symmetry. One may therefore write

$$\Delta F^{jp}(L) = \Delta F . e^{jp}_{A_{1g}}(L) \text{..... } (3.23)$$

where

$$e^{jp}_{A_{1g}}(L) = |A_{1g}>$$

is the unit vector of A_{1g} symmetry having components defined on the nearest neighbour sites. In this way

$$e^{jp}_{A_{1g}}(\pm R_0 J) = \pm 1/\sqrt{6}\delta_{jj},$$

if prefers to the nearest neighbour ions

=O, at all other sites.....(3.24)

and

$$F = -\left[V_1'(R_0+u) - V_0'(R_0)\right] \text{.....(3.25)}$$

The change in force vector, $\Delta F^{jp}(L)$, will be isolated by the assumed harmonic response of the rest of the lattice. Thus, at the equilibrium position

$$F^{jp}(L) - \left[\sum_{L'}\sum_{P'}\sum_{J'}\phi^{jj'}pp'(LL')u^{j'p'}(L') - correction\right] = 0 \text{ .....(3.26)}$$

Hence ϕ is the unperturbed coupling constant matrix in terms of the second derivatives of the potential energy V.

Introduction of the correction term becomes necessary because of the fact that the short range forces between the impurity and the nearest ions have already been taken into consideration. The correction term can be written as follows.

$$\text{Correction} = V_0'' u e^{jp}_{A_{1g}}(L) \text{ ..... (3.27)}$$

Let $\bar{\phi}$ represent the matrix with components $\bar{\phi}^{jj'}pp'(L)$ and $\bar{u}$ represent a column vector with the components u^{jp}(L).

Then using equation (3.23) and (3.27), the equilibrium condition (3.26) becomes.

$$\bar{u} = \bar{\phi}^{-1}\left|A_{1g}\right> \left(\Delta F + V_0^{''}u\right)$$

Thus,

$$u = \left\langle A_{1g}\middle|\bar{u}\right\rangle = \left\langle A_{1g}\middle|\bar{\phi}^{-1}\middle|A_{1g}\right\rangle \left(\Delta F + V_0^{''}u\right)$$

or,

$$u = \alpha_0 F_r = G_0\left(A_{1g}\right)/ M_H F_r \text{.....(3.28)}$$

where,

$$F_r = \left(\Delta F + V_0^{''}u\right)$$

In the equation (3.28), M_H is the mass of the nearest neighbour ion and $G_0(A_{1g})$ is the static Green's function of spherical symmetry. Equation (3.28) shows similarity of this method with that of Hardy[49].

3.4 Frequency of The Free OH^- ION Band- Center:

A knowledge of the free OH^- ion frequently is necessary in order to evaluate the shift of the stretching band-center of the matrix trapped OH^- ion. Unfortunately, there are no precise measurements or calculations for the stretching frequency of the free OH^- ion.

From photo detachment measurements, Branscomb[51] has estimated W_e for free OH^- ion as 3735+560cm^{-1}. Wedding and Klein[52] have given the value of w_ex_e for OH^- (in KBr matrix) as 85.8cm^{-1}.

This, with the Branscomb's[51] value of W_e, gives the free ion stretching frequency as 3564 cm^{-1} with the same uncertainty as reported for W_e by Branscomb (viz. $\pm 560 cm^{-1}$).

Cade[53] calculations have predicted the value of W_e for free OH^- ion to lie in the range 3733-3820cm^{-1} using this value for W_e and taking W_eX_e =85.5 cm^{-1}, Wedding and Klein[52] estimate the stretching frequency for free OH^- to lie in the range 3560-3650cm^{-1}. According to them, one generally expects the free ion stretching frequency to be lower than that for the ionic matrix trapped impurity ion.

Thus, the free OH^- ion frequency W should be less than 3603 cm^{-1} which is the lowest observed value of the stretching frequency in an alkali halide matrix[52].

The stretching frequency for free ion, neutal OH^0, has been given as 3569 cm^{-1}. Imposition of a change on the neutral OH^0 would soften the intermolecular force constant and reduce the stretching frequency.

Thus, an upper limit for the free OH^- ion frequency can be set at the value 3569cm^{-1} and the expected range is narrowed down to 3560-3569 cm^{-1}.

From the Buckingham's theory, the ratio $\Delta w/w$ for a given matrix material remains the same for the isotropically substituted impurities. Mann et. al.[54] have utilized this fact in dealing with the band center shift for HCl, DCl, HBr and DBr impurities trapped in the rare gas matrices.

Following the same line, we determining the stretching frequency for fee OH^- & OD^- ions as 3564.5 and 2628.8 cm^{-1} respectively.

Our estimated value of free OH^- ion stretching frequency lies well within the range provided in the above arguments by several other workers [51-53].

In our method of estimating the free OH^- ion stretching frequency the input data are the absorption frequencies of the OH^- ion trapped in alkali halide matrices. These are available with an uncertainty of $\pm 0.5 cm^{-1}$.[52]

Thus the uncertainty in our estimated value is much lower than that in those obtained from the data of Branscomb[51].

The isotropic- shift results obtained from our values are given in the table 3.1. These are also in good agreement with theory put an additional reliance on the correctness of our results.

Table-3.1

Effect of the isotropic substitution of shift of the band center of hydroxyl ion impurity in alkali halide matrices.

Matrix	**$\Delta w/w$ for OH^-**	**$\Delta w/w$ for OD^-**
KCl	0.0214	0.0211
KBr	0.0148	0.0148
NaCl	0.0255	0.0230
LiF	0.0467	0.0450

3.5 Results and Discussions:

Table (3.2) gives the values of the various constants used in the present calculations. Table (3.3) gives the calculated shifts of the band-center and compares it with the experimentally observed results. The total shift has been expressed as the sum of a red and a blue contribution, as already described. It can be seen from the table that the blue shift, corresponding to the repulsive interaction dominates over the red shift.

This is in qualitative agreement with the experimental results. For a quantitative discussion, it may be mentioned that the shifts are to be evaluated under the handicap of no precise information about the parameters A, B and C in equations (3.10) and (3.12).

Their values, therefore, are to be determined from the observed values of the shifts themselves. We use the shift data of LiF, NaF and NaCl matrices to obtain the parameters A,B and C by making use of the equation (3.10). These systems have been chosen because the lattice distortion in these cases is known. We have taken the OH^- ion as being equivalent to the isoelectric F^- ion. Thus, no lattice distortion is expected in LiF and NaF matrices.

Lattice distortion for the NaCl – OH^- (F^-) system in known for the Fukai's measurements of the quadrupolar broadening of NMR line[55]. These are obtained as A = 167-304, B = $-\ 8.1669\times10^{-16}$ and C = $+5.2359\times10^{-8}$ units. The fifth column of the table represents the shifts obtained for these and a number of other matrices with above mentioned values of the parameter A, B and C. It can be seen that such a calculation does not explain the observed shifts in a consistent manner.

The following causes can be attributed to this discrepancy:

1. The polarizability values of the captions and anions become increasingly uncertain for small inter-ionic separation[56]. As the parameters A, B and C have been obtained from the observed shifts in NaF, LiF and NaCl matrices, it is quite likely that the uncertain values of the polarizability in these cases might affect adversely the values of the parameters A,B, and C thereby giving an incorrect shift in the other systems also.

2. The localized lattice vibrations of the surrounding lattice points can also affect the position of the band- center. This effect has been found to be important in understanding the shift of the librational and tunneling levels

of these impurity matrix- systems [57,58]. When an impurity is added to the crystal, the near neighbouring atoms move to the new equilibrium positions, depending upon the host crystal matrix and the nature and size of the impurity. Such displacements have been found to of much importance in understanding the thermal conductivity measurements[50] and the quadrupolar broadening of the NMR lines[55]. More recently de Jong[59] has made the use of elastic relaxation of lattice around impurity ions substituted in KI matrix, in order to explain the frequency of the impurity induced gap modes. It is quite likely that these same elastic displacements of the nearest neibhrour atoms are responsible for the difference in the calculated and the observed shift of the band- center.

For the item (1) it can be said that the polarizability values affect only the red contribution of the shift. As can be seen from the table (3.3), this is just 1% of the total shift and hence any error in the polarizability values will not affect the results much. For the item (2), it has been observed that this effect is more important for the tunneling level than for the librational level[58]. It has been well realized, that larger the frequency of the motional state of the impurity, the smaller is the effect of the localized vibrations on it. The shift of the band-center is, therefore, not expected to be much affected by coupling with the localized lattice vibrations.

It is the third item, therefore, which is added to be the chief cause of the present disagreement between the calculated and the observed shifts. To evaluate this effect one should first calculate theoretically the isotropic displacement of the nearest neighbours of the impurity and then work out its effect on the position of the band- center.

However, we do it in the reverse way. Table (3.4) gives the value of the displacement of the nearest neighbours needed to fit the calculated shifts to the experimental values.

We have taken that OH^- ion as approximately spherical and equivalent to the fluoride ion which is isoelectronic to it. Thus, we have made use of the repulsive potential parameters of alkali fluorides for OH^- ions trapped in the alkali halide matrices[47], Recently, Ward and Timusk[60] have presented the experimental results of the impurity induced far-infrared absorption for KBr- OH^- and KBr-F^- systems. Both the systems have resonances at $37cm^{-1}$, and in general appearances the spectra of these systems are quite similar, as expected from a nearly similar electronic structure of these impurities. Also, in their theoretical calculations, Ward and Timusk[60] have used the same force constant for OH^- and F^- impurities. The lattice distortions around the impurity have also been calculated following the well-known method of Brauer[47] and Caldwell and Klein[50], separately.

The results of lattice distortion obtained experimentally by other workers[50,61] have also been given in the table (3.4) along with those obtained from the Brauer[47] and Caldwell and Klein's[50] methods. It can be seen that the lattice distortion needed to explain the observed shift, agree well with those calculated from the different models[47,50] and observed experimentally[50,61].

Table-3.2

The constants used in the calculations.

Systems	R_0^a **A⁰**	α_H^b A^{0^3}	r^a + A^0	r^a – A^0	ρ^a A^0	r_e^c A^0	$\left(\frac{d\mu_s}{d\gamma}\right) r_e^d$ A^0
KCl- OH^-	3.139	3.29	1.463	1.179	.338	.974	0.143
KBr- OH^-	3.293	3.29	,,	1.179	,,	,,	,,
KI- OH^-	3.526	3.29	,,	,,	,,	,,	,,
RbCl- OH^-	3.270	4.56	1.587	,,	.328	,,	,,
NaBr- OH^-	2.981	1.57	1.170	,,	.330	,,	,,

Systems	R_0^a **A⁰**	α_H^b A^{0^3}	$\overset{a}{r}$ + A^0	$\overset{a}{r}$ – A^0	$\overset{a}{\rho}$ A^0	$\overset{c}{r_e}$ A^0	$\left(\frac{d\mu_s}{d\gamma}\right)^d r_e$ A^0
NaCl- OH^-	2.814	,,	,,	,,	,,	,,	,,
NaF- OH^-	2.310	,,	,,	,,	,,	,,	,,
Lif- OH^-	2.010	1.00	0.816	,,	.299	,,	,,

a - Reference - 62

b - Reference - 63

c - Reference - 64

d - Reference - 52

Table-3.3

Calculated and observed values of the shift of the band-center, when lattice distrotion is not considered and when it is considered.

System	Observed shift of the band-center cm^{-1}	Calculated shift[A]			Calculated shift[B]		
		Red shift equation (3.5) cm^{-1}	Blue shift equation (3.6) cm^{-1}	Total Shift cm^{-1}	Red shift equation (3.5) cm^{-1}	Blue shift equation (3.6) cm^{-1}	Total Shift cm^{-1}
KCl- OH^-	76.5±0.5[a]	–.5	56.5	56.00	–.6	77.6	77.0
KBr- OH^-	53.0±0.5[a]	–.4	30.2	29.8	–.5	53.5	53.0
KI- OH^-	38.5±1.0[c]	–.2	6.7	6.5	–.3	38.8	38.5
RbCl- OH^-	68.0±0.5[d]	–.5	52.9	52.4	–.6	67.6	67.0
NaBr- OH^-	61.5± .5[a]	–.3	30.9	30.6	–.4	61.9	61.5

System	Observed shift of the band-center cm^{-1}	Calculated shift[A]			Calculated shift[B]		
		Red shift equation (3.5) cm^{-1}	Blue shift equation (3.6) cm^{-1}	Total Shift cm^{-1}	Red shift equation (3.5) cm^{-1}	Blue shift equation (3.6) cm^{-1}	Total Shift cm^{-1}
NaCl- OH^-	90.0±0.5[a]	–.5	90.5	90.0	–.6	90.6	90.0
NaF- OH^-	163.5[b]	–1.5	165.0	163.5	–1.5	165.0	163.0
Lif- OH^-	166.5[e]	–2.0	168.5	166.5	–2.0	168.0	166.5

A - When lattice distortion is not considered

B - When lattice distortion is considered.

a- Reference -52,

b- Reference -65,

c- Reference -66,

d- Reference -67,

e- Reference -68.

Table-3.3

Calculated and observed values of the shift of the band- center, when lattice distortion is not considered and when it is considered.

Systems	**Observed shift of the band-center cm^{-1}**	**Calculated shift**			**Calculated shift**		
		Red shift cm^{-1}	**Blue shift cm^{-1}**	**Total Shift cm^{-1}**	**Red shift cm^{-1}**	**Blue shift cm^{-1}**	**Total Shift cm^{-1}**
KCl- OD^-	55.7±.5[a]	–.4	41.1	40.8	–.4	56.5	56.1
KBr- OD^-	39.2±.5[a]	–.3	22.0	21.7	–.4	38.9	38.5
NaCl- OD^-	60.2[a]	–.4	65.9	65.3	–.4	65.9	65.5
Lif- OD^-	118.2[e]	–.4	122.7	121.2	–1.4	122.6	121.2

Table-3.4

Lattice distortion parameter required to explain the observed shift of the band-center (in OH^-/OD^- substituted alkali halide matrices) as compared with their calculated values on the basis of Brauers and Hardy's theoretical model or obtained from other experimental studies.

System	Percentage lattice distortion parameter			
	Required to explain the observed shift of the band-center	**Calculated from Brauers method[a]**	**Hardy's method as modified by Klein at al.[b]**	**Other experimental values.**
KCl- OH^-	–3.0	–3.0	–4.0	2.7[c]
KBr- OH^-	–4.2	–5.0	–4.2	-
KI- OH^-	8.2	–7.1	–3.6	-
RbCl- OH^-	–2.0	–2.3	–3.3	-
NaBr- OH^-	–5.6	–6.1	–6.2	-
NaCl- OH^-	–4.2	–5.2	6.5	4.2[d]
NaF- OH^-	0.0	0.0	0.0	-
Lif- OH^-	0.0	0.0	0.0	-

a- Reference -47,

b- Reference -49,50

c- Reference -61,

d- Reference -55.

ISBN: 978-81-949998-9-8

Chapter 4

Off-Centre Direction of Impurities in Alkali Halide Crystal Matrics

4.1 Introduction:

An accurate calculation of the barrier hindering angular motion of polar impurities in alkali halide crystal systems requires an adequate knowledge of the interaction between the impurity molecule and the ions of the host crystal matrix. The possible off-center displacement of the impurity's center of mass from the normal lattice site can be obtained by determining the minimum energy configuration of the combined impurity-matrix system. For rigorous determination of the off-center displacement, one requires to calculate the variation of the energy of the system as a function of the impurity's displacement. Such type of calculations have been done for Li^+ impurity trapped in alkali halide crystals for which the potential form is well known. Unfortunately, such potentials are not available for the dipolar impurity -host matrix ion systems, and hence the calculation of this type is very difficult to be done for the present systems.

The present calculation of the displaced position of the impurity center of mass (CM) is based on the multipole expansion method of the intermolecular interaction. The idea of possible off-center displacement of the CM of the dipolar impurity in alkali halide matrices was first suggested by Seward and Narayanamurti[69]. The reason for such a displacement can be stated as follows:

The equilibrium position of the impurity in the matrix cavity is described by the minimum energy configuration of the impurity matrix system. The interaction energy depends upon the distribution of charges in the dipolar impurity and that in the ions of the host matrix. Consequently, the point of the impurity that rests

at the normal lattice site in the minimum energy configuration will depend upon the distribution of charge and not upon the distribution of masses in the impurity. We call this point the center of interaction (CI), because it is this point at which the effective crystalline field interaction acts. Essentially, the CI need not coincide with the CM, because the latter is governed by the distribution of masses in the impurity. We assume that the angular anisotropy of interaction is also minimum about the center of interaction. Our assumptions are as follows:

1. The impurity occupies a substitutional site in the host matrix cage with its CI and not the CM at the normal lattice site.

2. The angular anisotropy of the interaction is minimum about the CI. The concept of CI has recently been introduced by a number of workers[70] and the parameter (Separation between the molecular CI and CM) has been demonstrated to be of much importance in understanding a number of molecular problems in the gaseous phase. Such a concept of molecular CI has to also lead to the understanding of the matrix spectra of HCl and HBr type of impurities in rare gas matrices at low temperatures.

So far as the properties of this CI are concerned, the following points may be mentioned.

1. Where there is a symmetric charge distribution in the molecule, the CI can be taken as located at the center of symmetry.

2. For an asymmetric charge distribution, CI is the point about which the angular dependence of the intermolecular interaction is minimum. The relative importance of various types of these interactions (like dispersion, induction, exchange and multipole interaction), which are not centered necessarily at the same point, is determined by the intermolecular distances and the environs of the impurity. The CI of an asymmetric molecule is,

therefore, not only a molecular constant but also depends upon the environment of the impurity. The position of the CI may also slightly depend upon the experimental conditions, such as temperature, pressure and state of aggregation etc. These latter small effects, however, will not be considered here.

4.2 Monoatomic Impurities in Solid State Matrices:

There are strong experimental as well as theoretical evidences for the off-centered position of certain monoatomic impurities doped in the alkali halide crystals. Electro-caloric measurements[27] and the dielectric measurements[28] have already established the existence of an off- centered positions for Li^+ ions doped in the KCl matrix. The measurement of velocity of sound and absorption by Byer and Sack[71] have showed that Li^+ ions is displaced in one of the eight <111> directions in the KCl crystal matrices. The more recent far-infrared absorption measurements of Kirby et.al. 72 for the KCl–Li^+ system, have given a value of the off-center displacement parameter 'a' as $1.2A^0$. For the RbCl–Ag^+ system, however, controversial results have been obtained by Kirby et.al.[72] and by Kaphan and Luty.[73] Kaphan and Luty could explain their para-electric cooling results on the basis of a <111> displacement directions for Ag^+ ion in RbCl matrix, whereas the multiplet structure of the far-infrared[72] absorption ruled out such a configuration and presented evidences for a displacement in <110> direction.

The theoretical calculations of Wilson et.al.[82] have predicted an off-centered displacement for the Li^+ ion in the NaCl matrix. The far-infrared absorption measurements by Kirby et.al.[72] suggest that the Li^+ impurity may have a central instability in the NaCl matrix. However, neither para- electric cooling nor tunneling effect in the para-elecric resonance has been observed for this system to give a definite proof of an off-centered configuration.

4.3 Determination of The Off-Center Direction:

There are different theoretical models for the calculation of off- centered displacement and direction of the impurity ion in the crystal matrices. The methods of Quigley[56] and that of Wilson et.al.[82] determine the minimum energy configuration of the entire impurity crystal matrix system in different crystallographic directions. These calculations employ a polarizable point-ion model for the crystal and use generalized or some modified form of Born-Mayer potential for the repulsive interactions.

Our method of approach is quite simple and determinations only the direction of the off-centered impurity ion. In analogy with the diatomic impurities can be pictured as performing a quasi-rotational motion with the moment of inertia.

$I = m a^2$, where a is the off-centered displacement of the impurity from the normal lattice site. Our method works on the calculation of certain barrier parameters for the quasi-rotational motion of the impurity ion.

The angle dependent part of the crystalline-field potential at the impurity site will naturally have the octahedral symmetry. In the Devonshire model[32], only the first significant angle dependent term (L = 4cm) is retained in the expansion of the octahedral potential in terms of spherical harmonics. The Devonshire potential in its simplest form can be written as:

$$V(\theta,\phi)=V_4= K(\mathrm{Sin}^4\theta.\ \mathrm{Sin}^2\phi.\ \mathrm{Cos}^2\phi+\mathrm{Sin}^2\theta.\mathrm{Cos}^2\theta) \ldots.(4.1)$$

Where K is a barrier parameter.

It is well known that a positive K value gives a <100> equilibrium orientation to the impurity ion, whereas a negative K value gives a <111> equilibrium configuration. A <110> off-centered direction cannot be thought of in terms of the simple Deovnshire potential. Recently, it has been shown that a <110>

equilibrium orientation can be visualized only if one adds a large V_6(L=6) term to the Devonshire octahedral potential[32]. This generalized potential then can be expresed as:

$$V(\theta, \phi) = V_4 + V_6$$

$$= K(\mathrm{Sin}^4\theta . \mathrm{Sin}^2\phi \, \mathrm{Cos}^2\phi + \mathrm{Sin}^2\theta \mathrm{Cos}^2\theta)$$

$$+ K'[\mathrm{Sin}^6\theta (\mathrm{Cos}^6\phi + \mathrm{Sin}^6\phi) + \mathrm{Cos}^6\theta)] \quad \ldots\ldots\ldots\ldots (4.2)$$

where K is a Devonshire barrier parameter and K' is an additional barrier parameter.

Further, it has been shown[75] that if the ratio K/K' lies between 3.0 and 1.5, the minimum energy configuration of the impurity will be along the <100> direction. Otherwise it will be along <111> or <100> direction depending upon the sign of the Devonshire barrier parameter K. In our method of calculation, we calculate only these barrier parameters on the basis of a simple model and determine from the ratio of K/K' or the sign of the parameter K, the equilibrium orientation direction of the impurity ion in the crystal matrix.

For calculating the barrier parameter K and K', one can use either of the two specific models:

(i) Point- charge- point- dipole model, introduced by Lawless.[63]

(ii) Multipole- expansion model recently developed by Pandey et.al. 64

For the case of atomic impurities with no intrinsic dipole moment, both the models give an identical result. A simple calculation yields the following results for the parameter K and K' as follows:

$$K = \frac{C_H C_S}{R}\left\{\left[\frac{35}{2^2}\left(\frac{a}{R}\right)^4 + \frac{3465}{2^5}(a/2)^8\right]\right.$$

Ist Shell

$$+\left[\frac{35}{2^3 3^4}(a/R)^4 + \frac{3465}{2^6 3^6}(a/R)^8\right]$$

2nd Shell

+ similar terms for the next shells}

$$+\frac{\alpha_H C_S^2 + \alpha_S C_H^2}{R^4}\left\{\left[5.2^4(a/R)^4 + 105.2^4(a/R)^8\right]\right.$$

Ist Shell

+ Similar terms for the next shells }

$$K' = \frac{C_H C_S}{R}\left\{\left[\frac{231}{2^3}(a/R)^6\right]\right. \quad + \quad \left[\frac{231}{2^4 3^6}(a/R)^6\right]$$

Ist Shell 2nd Shell

+ Similar terms for the next shells }

$$+\frac{\alpha_H C_S^2 + \alpha_S C_H^2}{R^4}\left\{\left[7.2^7(a/R)^6\right]\right.$$

1st shell

+ Similar terms for the next shells.}.....(4.3)

Here, R is the lattice constant of the host crystal and 'a' is the off- center displacement of the impurity in the host matrix. C and α represent the charge and

total polarizability respectively. The constants used in the calculations are tabulated in the table (4.1).

4.4 Results and Discussions:

In fig. (4.1) we report that calculation of the ratio K/K' as a function of the off-centered displacement parameter 'a'. In the same fig., we have marked the regions for the <111> and the <110> orientation based on the calculation of Mitra et al.[75]. In our calculation we have considered different summations upto the fourth neighbouring shell of the impurity.

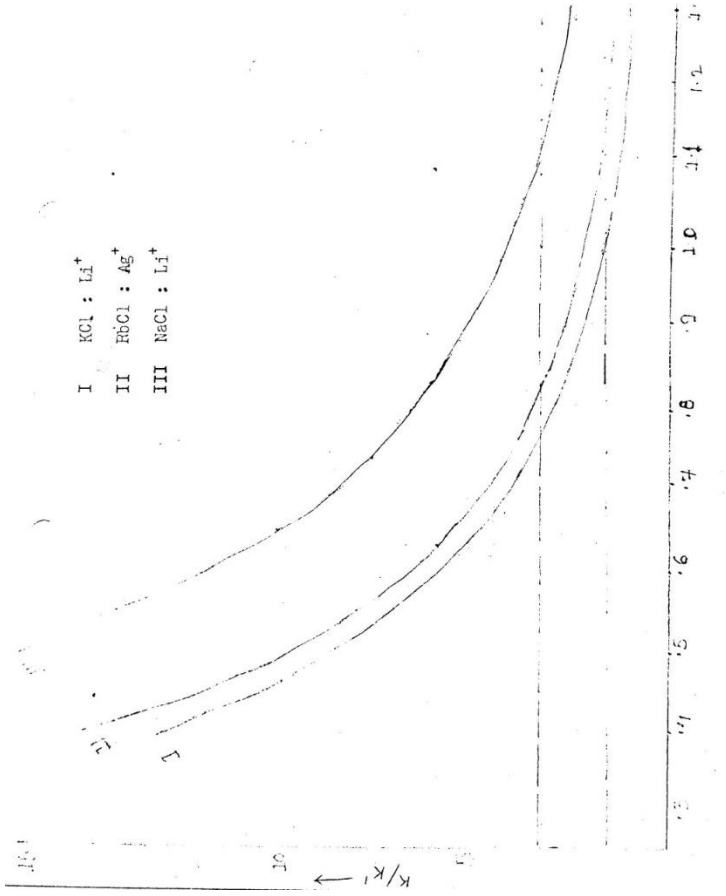

Fig. 4.1, Ratio K/K' as a function of 'a'

Table-4.1

Constants used in the calculation of the parameters K and K'.

System	Lattice Parameter R (A^0)	$\alpha_H^{b+}(A^{03})$	$\alpha_H^{b-}(A^{03})$	$\alpha_S^{b+}(A^{03})$
KCl–Li^+	3.139	3.29	4.98	1.00
NaCl–Li^+	2.814	1.57	4.98	1.00
RbCl–Ag^+	3.270	4.56	4.98	3.13

a - Reference - 62

b - Reference - 63

For the RbCl –Ag^+ system, it can be seen (4.1) that if the off- center position exceeds the value of $0.82A^0$, a <110> direction of displacement becomes more probable. The experimentally observed value of this parameter for RbCl– Ag^+ system is $0.83 \pm .08$ $A^{0\,72}$, establishing the fact that probably it is an example of a boarder- line case. This can explain the reason of the controversy between the two authors[72,73] and our calculations of K/K' for highly ordered crystal matrices. Dislocations and other imperfects near the impurity may stabilize either of the orientations. Hence the reason of the controversy may be attached to the use of improperly grown crystals and to the fact that this is an example of boarder-line case between <111> and <110> orientations.

Large amount of the internal strain or internal electric fields are always present in a normal crystal. These have also been found to be responsible for the large line widths observed in the paraelectric resonance experiments and for the form of the specific heat anomaly of the paraelectrics. More recently Timme et.al.[78] have done paraelectric spectroscopy experiments on KCl^- Li^+ system with

different crystal orientations. Their results have been found to be in serious disagreement with the simple <111> model. They have observed the existence of two lines for certain crystal orientations, where only one is expected from the <111> model. Moreover, for certain other crystal orientations, they observe only one line whereas the <111> model predicts two lines to be observed. They explained the anomalous spectral features by incorporating the large internal strains in the crystal matrix around the impurity. Very recently Kaphan and Luty[79] have carried out a detailed study of the static and dynamic para-electric behaviour of Ag^+ ion in RbCl and RbBr matrices, using the electrodichroism of Ag^+ ultraviolet band. The static electro-optical measurements reveal a <110> orientation with the dipole moment value of $0.78A^0$ for RbCl–Ag^+ system.

The dynamical, time dependent electrodichroism measurements show the presence of two different relaxation processes for this system. This behaviour could be understood only in terms of a strong E_g distortion of the lattice. The off-centered displacement value of $0.78A^0$, though lies in <111> region, is quite near to the border line fig. (4.1).

In order to present the exact picture, perhaps, also the Eg distortion term is needed to be considered in the modified Devonshire potential equation (4.2). Our results for the RbCl–Ag^+ system can also be compared with those of the experimental and theoretical studies of certain other workers [80,82] and Dreybroadt and Fussgaenger[80] have observed the temperature dependence of the dipole strength of the $(4a)^{10} \rightarrow (4a)^9$ 5s electronic transition of the Ag^+ ion in the RbCl matrix. They also conclude that Ag^+ ion sits in an off- centered position in the RbCl matrix. Their subsequent calculations indicate that the impurity is off-centered by about $0.25A^0$ in the <111> crystallographic direction. From figure (4.1) it can be seen that our calculations also present a <111> off-centered direction for a = $0.25A^0$. A more recent calculation of Wilson et.al.[82] gives the off-centered

displacement position .54 A^0 in the <111> direction. This is also consistent with our calculations (Fig. 4.1).

For the sake of completeness, we are also presenting the calculations for KCl–Li^+ and NaCl –Li^+ systems and determining the off-centered directions in these cases as well. For the KCl-Li^+ figure (4.1) shows that for a value of 'a' greater than 1.08A^0, a <111> off centered position is plausible. The experimental value of the parameter 'a' is 1.2 A^0 [72], which predicts a <111> direction of displacement. This is in agreement with many experimental results[72,81]. For the NaCl–Li+ system, a <110> direction can be predicted only if 'a' becomes greater than 1.12A^0. Such a high value of displacement parameter 'a' in a NaCl matrix (Lattice constant = 2.81A^0) is highly improbable. Hence, in this system also a <111> direction of the off-centered displacement is expected (if is an off-center system at all). This is also in agreement with the results of Wilson et.al.[82]

ISBN: 978-81-949998-9-8

5. Conclusion

5.1 Conclusion:

Recently, keen interests have been devoted to study the rotational motion of molecules in solids of the alkali halide crystals doped with polar impurities at liquid helium/liquid nitrogen temperatures. Even a small concentration of these impurities shows pronounced effects on the optical, thermal and electrical properties of the host crystals. The introduction of the impurity in the crystal systems destroys the order of periodic symmetry of the crystal systems, which in turn modify thereby the normal modes of vibrations of the crystal from its usual plane wave form. Of course, the change is greatest in the vicinity of the defects. In addition to the effect of the impurity on the macroscopic properties of the host crystal, the purities themselves may have many characteristics that make them worthy of study in their own right.

Infrared absorption, thermal conductivity, specific heat, shift of the intermolecular vibrational line (band center) and off-centered displacement are the best key tools for the problem of rotational motion of molecules in solids has been studied using CN^{-}, OH^{-} and Li^{+} ions substituted for the halogen in KCl, KBr, KI, RbCl, NaCl and NaBr. Every levels associated with the ion performing free rotation hindered rotation, oscillation, librational and tunneling motions were observed. It was found that a simple 3-dimensional potential for a linear diatomic molecule developed by Devonshire based on a 2-dimensional cosine potential first proposed by Pauling explained all of our observations. For the potassium halides the barrier height is 0.003, ev, in RbCl it is 0.0075 ev and in the sodium halides it is greater than 0.015 ev. Stress experiments show that the ion has six equilibrium orientations along the <100> directions.

At low temperatures ($kT << V_0$) the infrared spectrum should consist of a strong Q branch with weak satellites separated from the fundamental by multiples of the librational frequency. At high temperatures ($kT>V_0$) the spectrum should approximate that known for free molecules i.e., it should consist of P and R branches with a missing Q central branch. For intermediate temperatures ($kT\approx V_0$) the spectrum should consist of P, Q and R branches of comparable intensity. In quantum mechanical discussion of the states of rotational motion with the semi-classical picture of a rotating molecule one can describe the states below the barrier V_0 as oscillatory motions of the molecule in a particular well. This does not imply that in these states the molecule cannot move from one well to another. Such a change of the orientation is of particular interest if the influence of an electric stress field is studied. This description fails if the reorientation takes place through a tunnel process which is purely quantum mechanical.

A qualitative comparison of the KCl and KBr data with the selection rules indicates that below 20^0K the motion of the molecule can best be described as librational. Between 20 to 50^0K the molecule performs hindered rotational motion i.e., in this temperature's region a significant number of molecules occupy energy states both above and below the barrier. Above 60^0K most of the molecules occupy energy states lying above the barrier and now the characteristic P and R maxima of free molecules are observed. Fig. (1.15) shows that the separation of the P and R maxima follow a $T^{\frac{1}{2}}$ law predicted by equation (1.5). From these data the rotational constant $\tilde{B} = 1.25\,\mathrm{cm}^{-1}$ is obtained for the KCl host lattice. From $\tilde{B}$ the moment of inertia I and hence the internuclear separation between the C and N atoms is calculated to $r = 1.4A^0$.

Pauling has estimated that the radii of the carbon and nitrogen atoms to be 0.7 and $0.77A^0$ from which a maximum value of 1.47 for the C–N bond length may be reduced.

Recently Elliot and Hastings have used $1.16A^0$ for the C–N bond length in pure KCN in order to fit their neutron-diffraction data. Considering the simplicity of the model used the agreement between the calculated and the experiment is considered very satisfactory.

The infrared measurement on CN^- in KCl, KBr, KI and RbCl have shown that at high temperatures the molecules can rotate freely in the lattice. At low temperatures the molecules perform librational motion with a frequency of 11 to $12cm^{-1}$ in potassium halides and about $19cm^{-1}$ in RbCl. In addition uniaxial-stress measurements show that in these host lattices the CN^- can reorient down to the lowest temperature of our measurement (1.36^0K), the minima in the potential function being the <100> directions. In NaCl and NaBr the CN^- is locked in at low temperatures and the barrier hindering rotation is estimated to be greater than 100 cm^{-1}. Finally, the energy levels of the CN^- in a six-well potential have been quantitatively considered for the potassium halides and RbCl in terms of Devonshire model. This model can explain a number of features of the IR data but predicts tunneling transitions which were not observed in optical measurements, discussed in chapter one.

CHAPTER second deals with the thermal conductivity and specific heat of CN^- doped alkali halide crystals by phonon spectroscopy. The questions posed by optical spectroscopy can satisfactorily be answered by thermal conductivity of KCl, KBr and NaCl and specific heat of KCl: CN measurements. Strong phonon scattering by tunneling and rotational states is observed. The scattering can be quantitatively described with a Lorenazian resonance cross- section.

From fig. (2.4) we see that at low temperatures the CN^- has no effect. The depression at 40^0K may be caused by scattering of the CN^- both as a molecule and as a point defect. Similar high temperature depressions have been observed

in the thermal conductivity of crystals containing about the same concentration of monatomic defects. Assuming that the scattering is caused by rotational states of the CN^- lying at the top of the potential barrier we calculate the barrier height to be 140 cm^{-1} from the position of the dip in the thermal conductivity, which is in agreement with the IR data.

A comparison of the KCl and KBr data shows that such simple picture is inadequate. Instead one must calculate the field dependence of the energy levels, fig. (2.2) and it is conceivable that this would be different for the two host lattices. It appears that experiments of this kind can provide a better understanding of the lowest energy states of the molecules in solids.

Fig. (2.5) gives the measured specific heat of KCl:CN. The graph shows dramatically the size of the anomaly relative to the size of the lattice specific heat, curve D. In order to analyse the anomaly the lattice specific heat must be subtracted. fig. (2.6). The theoretical curve I, calculated from equation (2.6) using the energies and degeneracies from equation (2.2), is the expected Schottky specific heat for the sample (B). Curves (B) & (C) exhibit the same shape below 1.5^0K indicating that the level spacing is in reasonable agreement with the prediction but both curves are broader than the calculated curves. The broadening is attributed to the residual strain in the crystal.

The experimental methods described above have resulted in a detailed picture of the rotational degrees of freedoms of the molecular impurity CN^- in a variety of alkali halide host lattices. This picture is in excellent agreement with the model proposed by Pauling as refined by Devonshire. The potential barrier allows free motion above 60^0K in potassium salts and above 150^0K in the rubidium salt. In sodium salts finally even at 300^0K no free rotation is observed. At temperatures sufficiently below the ones mentioned the molecules perform librational motions, and at intermediate temperatures the motion can be described with the classical

picture of hindered rotation. The libration levels are split due to tunneling, and specific heat measurement show that this tunnel splitting is in complete agreement with the theory. It was also found that the rotational and the tunneling states couple strongly to the phonon, whereas the librational states do not. The phonon- scattering cross- sections have a Lorentzian resonance form. The phonon- molecule interaction is assumed to be through stress coupling which has been shown to be large from stress-induced alignment experiments. In the KBr and KI host lattice an additional center of mass motions of the CN^- ions appear likely. This type of motion had not been considered in the Pauling model. On the other hand a central instability should certainly be expected for cavities considerably larger than the impurity ion.

CHAPTER three throws light on the shift of the intramolecular vibrational line of OH^- impurity in alkali halide crystals. We have tried to explain the shift of the intramolecular vibrational absorption of the impurity in different alkali halide crystals on Buckingham's theory. This theory can very well account for the observed shift of the band center of OH^- and OD^- impurity in alkali halide matrices provided proper lattice distortion around the impurity is suitably considered. The amount of the lattice distortion needed to explain the observed shift agrees well with that obtained on the basis of Brauer method of calculating lattice distortion.

When a polyatomic impurity molecule is substituted in a crystal matrix, the molecular interactions between the impurity and the host matrix ions modify the stretching or bending vibrational spectra of the impurity. A systematic study of these spectral features can yield much informations about the molecular as well as intramolecular forces.

Table (3.3) gives the calculated shifts of the band-center and compares it with the experimentally observed results. The total shift has been expressed as the sum of

a red and a blue contribution, as already described. It can be seen from the table that the blue shift, corresponding to the repulsive interaction dominates over the red shift. This is in qualitative agreement with the experimental results. For a quantitative discussion, it may be mentioned that the shifts are to be evaluated under the handicap of no precise information about the parameters A, B and C in equations (3.10) and (3.12). Their values, therefore, are to be determined from the observed values of the shifts themselves. We use the shift data of LiF, NaF and NaCl matrices to obtain the parameters A,B and C by making use of the equatium (3.10). These are obtained as A = 167–304, B = -8.1669×10^{-16} and C = $+5.02359\times10^{-8}$ units. The fifth column of the Table (3.3) represents the shifts obtained for these and a number of other matrices with above mentioned values of the parameter A, B and C. It can be seen that such a calculation does not explain the observed shifts in a consistent manner. The following causes can be attributed to this discrepancy:

1. The polarizability values of the cations and anions become increasingly uncertain for small inter-ionic separation. As the parameters A, B and C have been obtained from the observed shifts in NaF, LiF and NaCl matrices, it is quite likely that the uncertain values of the polarizability in these cases might affect adversely the values of the parameters A, B and C thereby giving an incorrect shift in the other systems also.
2. The localized lattice vibrations of the surrounding lattice points can also affect the position of the band-center. This effect has been found to be important in understanding the shift of the librational and tunneling Levels of these impurity matrix- systems. When on impurity is added to the cyrstal, the near neighbours atoms move to the new equilibrium positions, depending upon the host crystal matrix and the nature ans size of the impurity. Such displacements have been found to of much improtance in understanding the thermal conductivity measurements and the quadrupolar

broadening of the NMR lines. More recently de Jong has made the use of elestic relaxation of lattice around impurity ions susbstituted in KI matrix, in order to explain the frequency of the impurity indueced gap modes. It is quite likely that these same elastic displacements of the nearest neighbour atoms are responsible for the difference in the calculated and the observed shift of the band- center.

For the (i) it can be said that the polarizability values affect only the red contribution of the shift. As can be seen from the table (3.3), this is just one percent of the total shift and hence any error in the polarizability values wll not affect the results much. For the item (ii), it has been observed that this effect is more important for the tunneling level than for the librational level. It has been well realised, that larger the frequency of the motional state of the impurity, the smaller is the effect of the localized vitrations on it. The shift of the band-center is, therefore, not expected to be much affected by coupling with the localized lattice vibrations.

It is the third item, therefore, which is added to be the chief cause of the present disagreement between the calculated and the observed shifts. To evaluate this effect one should first calculate theoretically the isotropic displacement of the nearest neighbours of the impurity and then work out its effect on the position of the band-center. However, we do it in the reverse way. Table (3.4) gives the value of the displacement of the nearest neighbours needed to fit the calculated shifts to the experimental values.

We have taken the OH^- ion as approximately spherical and equivalent to the fluoride ion which is isoelectronic to it. Thus, we have made use of the repulsive potential parameters of alkali fluorides for OH^- ions trapped in the alkali halide matrices. Recently Ward and Timusk have presented the experimented results of the impurity induced far-infrared absorption for KBr–OH^- and KBr–F^- systems.

Both the systems have resonances at $37cm^{-1}$ and in general appearances the spectra of these systems are quite similar, as expected from a nearly similar electronic structure of these impurities. Also in their theoretical calculations, Ward and Timusk have used the same force constant for OH^- and F^- impurities. The lattice distortions around the impurity have also been calculated following the well known method of Brauer and Caldwell and Klein, separately. The results of lattice distortion obtained experimentally by other workers have also been given in the table (3.4) along with those obtained from the Brauer and Caldwell and Klein's methods. It can be seen that the lattice distortion needed to explain the observed shift, agree well with those calculated from the different models and observed experimentally.

CHAPTER -IV determines the of-center direction of impurities (Li^+ & Ag^+) in alkali halide crystals. The possible of-center displacement of impurity's centre of mass from the normal lattice site can be obtained by determining the minimum energy configuration of the combined impurity-matrix system. The possible of-center displacement of the impurity's center of mass from the normal lattice site can be obtained by determining the minimum energy configuration of the combined impurity-matrix system. For rigorous determination of the of-center displacement, one requires to calculate the variation of the energy of the system as a function of the impurity's displacement.

The present calculation of the displaced position of the impurity center of mass (CM) is based on the multipole expansion method of the intermolecular interaction. The idea of possible of-center, displacement of the CM of the dipolar impurity in alkali halide matrices was first suggested by Seward and Nrayanamurti.

The equilibrium position of the impurity in the matrix cavity is described by the minimum energy configuration of the impurity matrix system. The interaction

energy depends upon the distribution of charges in the dipolar impurity and that in the ions of the host matrix. Consequently, the point of the impurity that rests at the normal lattice site in the minimum energy configuration will depend upon the distribution of charge and not upon the distribution of masses in the impurity. We call this point the center of interaction (CI), because it is this point at which the effective crystalline field interaction acts. Essentially, the CI need not coincide with the CM, because the latter is governed by the distribution of masses in the impurity. We assume that the angular anisotropy of interaction is also minimum about the center of interaction. So far as the properties of this CI are concerned, the following points may be mentioned:

1. Where there is a symmetric charge distribution in the molecule, the CI can be taken as located at the center of symmetry.

2. For an asymmetric charge distribution, CI is the point about which the angular dependence of the intermolecular interaction is minimum. The relative importance of various types of these interactions (like dispersion, induction, exchange and multipole interaction), which are not centered necessarily at the same point, is determined by the intermolecular distances and the environs of the impurity.

The CI of asymmetric molecule is, therefore, not only a molecular constant but also depends upon the environment of the impurity. The position of the CI may also slightly depend upon the experimental conditions, such as temperature, pressure and state of aggregation etc. These latter small effects, however, will not be considered here. In fig. (4.1) we report calculation of the ratio K/K' as a function of the off-centered displacement parameter 'a'. In the same fig. we have marked the regions for the <111> and the <110> orientations based on the calculation of Mitra et.al. For the RbCl-Ag^{+} system, it can be seen (4.1) that if the of-center position exceeds the value of $0.82A^{0}$, <110> direction of displacement

becomes more probable. The experimentally observed value of this parameter for RbCl-Ag+ system is 0.83± .08A^0 establishing the fact that probably it is an example of a boarder-line case. This can explain the reason of the controversy between the two authors and our calculations of K/K' for highly ordered crystal matrices. Dislocations and other imperfects near the impurity may stabilize either of the orientations. Hence the reason of the controversy may be attached to the use of improperly grown crystals and to the fact that this is an example of boarder-line case between <111> and <110> orientations.

Large amount of internal strain or internal electric fields are always present in a normal crystal. These have also been found to be responsible for the large line widths observed in the paraelectric resonance experiments and for the form of the specific heat anomaly of the paraelectrics. More recently Timme et.al. have done paraelectric spectroscopy experiments on KCl–Li^+ system with different crystal orientations. Their results have been found to be in serious disagreement with the simple <111> model. They have observed the existence of two lines for certain crystal orientations, where only one is expected from the <111> model. Moreover, for certain other crystal orientations, they observe only one line whereas the <111> model predicts two lines to be observed. They explained the anomalous spectral features by incorporating the large internal strains in the crystal matrix around the impurity. Very recently Kaphan and Luty have carried out a detailed study of the static and dynamic para electric behaviour of Ag^+ ion in RbCl and RbBr matrices, using the electrodichroism of Ag^+ ultraviolet band. The static electro-optical measurements reveal a <110> orientation with thte dipole moment value of 0.78 A^0 for RbCl–Ag^+ system.

The dynamical, time dependent electrodichroism measurements show the presence of two different relaxation processes for this system. This behaviour could be understood only in terms of a strong Eg distortion of the lattice. The off-

centered displacement value of $0.78A^0$, though lies in <111> region, is quite near to the border line, fig. (4.1).

In order to present the exact picture, perhaps, also the Eg distortion term is needed to be considered in the modified Devonshire potential equation (4.2). Our results of the RbCl–Ag^+ system can also be compared with those of the experimental and theoretical studies of certain other workers and Dreybrodt and Fussgaenger have observed the temperature dependence of the dipole strength of the $(4a)^{10} \rightarrow (4a)^9$ 5s electronic transition of the Ag+ ion in the RbCl matrix. They also conclude that Ag+ ion sits in an off-centered position in the RbCl matrix. Their subsequent calculations indicate that the impurity is off-centered by about $0.25A^0$ in the <111> crystallographic direction. From fig. (4.1) it can be seen that our calculations also present a <111> off-centered direction for a = $0.25A^0$. A more recent calculation of Wilson et.al. gives the off-centered displacement position $.54A^0$ in the <111> direction. This is also consistent with our calculations (fig.4.1).

For the sake of completeness, we are also presenting the calculations for KCl–Li^+ and NaCl–Li^+ systems and determining the off-centered directions in these cases as well. For the KCl- Li^+ Fig. (4.1) shows that for a value of 'a' greater than $1.08A^0$, a <111> off-centered position is plausible. The experimental value of the parameter 'a' is $1.2A^0$, which predicts a <111> direction of displacement. This is in agreement with many experimental results. For the NaCl–Li^+ system, a <110> direction can be predicted only if 'a' becomes greater than $1.12A^0$. Such a high value of displacement parameter 'a' in a NaCl matrix (Lattice constant = $2.81A^0$) is highly improbable. Hence, in this system also a <111> direction of the off-center displacement is expected (if it is an off-center system at all). This is also in agreement with the results of Wilson et.al.

ISBN: 978-81-949998-9-8

6. References

6.1 References:

01. Klein, M.V. : Phys. Rev. 122, 1393 (1961)

02. Klein, M.V. : Bull. Am. Soc. 10, 1348 (1965)

03. Klein, M.V. : Bull. Am. Phys. Soc. 8, 230 (1963)

04. Narayanamurti, V., Seward, W.D. and Pohl, R.O. : Phys. Rev. 148, 481 (1966)

05. Pohl, R.O. : Phys. Rev. Letters 8,481 (1962) and Z. physik. 176, 358, (1963)

06. Seward, W.D. : Proceeding of the Ninth International Conference on Low Temperature Physics Columbus Ohio, 1964, Edited by J.G. Daunt et.al., Plenum Press, Inc. New York, p.1130, (1965).

07. Narayanamurti,V. : Phy. Rev. Letters 13, 6, 93 (1964).

08. Narayanamurti,V. : Bull Am. Phys. Soc. 10, 390, (1965).

09. Narayanamurti,V. & Pohl, R.O. : Ibid. 10, 616 (1965).

10. Seward, W.D. : Ibid. 10, 617 (1965).

11. Roberts, V. : In. Sci. Instr. 31, 251, (1954), 32, 294, (1955).

12. Slack, G.A. : Phys. Rev. 105, 832, (1957).

13. Williams, W.S. : Phys. Rev. 119, 1021, (1960).

14. Keeson, P.H. and Pearlman, N. : Phys. Rev. 19, 1354, (1953).

15. Akpinar, S. : Ann. Physik, 37, 429 (1940).
16. Rolfe, J. Lipsett, F.R. and King, W.J. : Phys. Rev. 123, 447, (1961).
17. Gruzensky, M & Scott., A.B. : Phys. Chem. Solids. 21, 128, (1963).
18. Rolfe, J. : Bull. Am. Phys. Soc. 9. 227 (1964).

    Can. J. Phys. 42, 2195 (1964).
19. Fritz, B.; Luty, F. and Anger, J. : Z. Physik. 174, 240, (1963).
20. Pauling, L. : Phys. Rev. 36, 430, (1930).
21. Hexter, R.M. and Dows, D.A. : J.Chem. Phys. 25, 504 (1956).
22. Herberg, G. : "Molecular spectra & Molecular Structure", D. Van Norstrud Company, New York (1950) 2nd ed. Vol. 1.
23. Pauling, L. : 'Nature of Chemical Bond", Cornell University Press ithaca, New York, 1948, 2nd ed. p. 164.
24. Elliot, N. & Hastings, J. : Act. Cryst. 14, 1018 (1961).
25. Lytte, C.D. & A.J. Sievers : Bull Am. Phys. Soc. 10, 616, (1965).
26. Sievers, A.J.Maradudin, A.A., & Jaswal, S.S. : Phys. Rev. 138, A272, (1965).

27. Lambardo, G. & Pohl, R.O. : Phys. Rev. letters 15, 291, (1965).
28. Sack, H.S. & Moriarty, C.M. : Solid State Commun. 3, 93 (1965).
29. Silsbee, R.H. : Phys. Rev. 138, A180, (1965).
30. Sussmann, J.A. : J. Phys. Kondensierten materie 2 479, (1964).
31. Kazing, W. : Phys. Chem. Solids. 23, 479 (1964).
32. Devonshire, A.F. : Proc. Roy., Soc. (London) A153, 601, (1936).
33. Tinkham, M. : Group theory of quantum mechanics McGraw- Hill Book Company, New York, (1964).
34. Callaway, J. : Phys. Rev. 113, 1046, (1959).
35. Pohl, R.O. : Z. Physik. 176, 358 (1963).
36. Berman, R. and Brock, J.C.F. : Proc. Roy. Soc. (London), A 289, 46 (1965).
37. Walker, C.T. and Pohl, R.O. : Phys. Rev. 131, 1433, (1965).
38. Griffin, A. and Carruthers. : Phys. Rev. 131, 1976, (1965).
39. Wagner, M. : Phys. Rev. 131, 1443, (1963).
40. Wagner, M. : Phys. Rev. 131, 2520, (1963); 133, A750 (1962).
41. Sussmann, J.A. : Phys. Kondensierten materie 2 479,(1964).
42. Rosenberg, H.M. : "Low temperature solid state physics". Oxford University Press, Oxford. (1963).
43. Shepher, I. & Feher. G : Phys. Rev. Letters 15, 194, (1965).

44. Brout, R. : Phys. Rev. Letters 14, 195, (1965).

45. Roberts, J. S. Kanzig, W. & Hart, H.R. : Phys. Rev. Letters 13, 543, (1964).

46. Buckingham, A.D. : Proc. Roy. Soc. (London) 249, 169 (1958)

47. Brauer, P.Z. : Nature forsch, 79, 372, (1952)

48. Kanzaki, H. : J. Phys. Chem. Solids 2, 24, 107 (1957)

49. Hardy, J.R. : J. Phys. Chem. Solids 15, 39 (1960)

Ibid. 23, 113 (1962)

50. Caldwell, R.F. and Klein, M.V. : Phys. Rev. 158, 851, (1967).

51. Branscomb, L.M. : Phys. Rev. 148, 11, (1960).

52. Wedding, B. and Klein, M.V. : Phys. Rev. 177, 1274, (1969).

53. Cade, P. : J. Chem. Phy. 47, 2390, (1967).

54. Mann, D.E., A.C. Quista N. Ac. & White, D. : J. Chem. Phy. 44, 3453, (1960).

55. Fukai, Y. : J. Phy. Soc. (Japan) 18, 1580, (1963).

56. Quigley, R.J. and Das, T.P. : Phys. Rev. 164, 1185, (1967).

57. Pandey, G.K., : J. Chem. Phy. 49, 1555, (1908).

58. Pandey, G.K. and Agrawal, V.K. : J. Chem. Phy. 50, 1935, (1969).

59. De Jong, C. : Solid state Commun. 9,527, (1971).

60. Ward, R.W. and Timusk, T. : Phys. Rev. B5, 2351, (1972).

61. Hartel. H. and Luty, F. : Phys. States Solid 12, 347, (1965).

62. Tosi, M.P. and Fumi F.G. : Phys. Chem. Solids 25 45 (1964).

63. Lawless, W.N. : J. Phys. Chem. Solids 28, 1755, (1967).

64. Pandey, G.K. and Shukla, D.K. : Phys. Rev. B3, 4391, (1971)

65. Meisrich, M.L. : J. Phys. Chem. Solids 29, 1119, (1968).

66. Stoebe, T.G. : J. Phys. Chem. Solids 28, 1375, (1967).

67. Fenner, W.R. and Kelin, M.V. : "Light Scattering Spectrum of Solids". edit. by Wright G.B. (Springer Verlag, New York, 1969, Paper No F6, .497.

68. Guckelsberger, K.; Neumaier, K. and Zelsman, H.R. : Phys. Lett. 31A, 397 (1970).

69. Seward, W.D. and Narayanmurti, V. : Phys. Rev. 148,463 (1966).

70. Babloyantz, A.; Bellermans. A. Friedman, H. : Mod. Phys. 2 39 (1959).

Nuovo cimento 9, 181 (1958)

Adv. Chem. Phys. 4, 225 (1962).

71. Byer, N.E. & Sack, H.S. : J. Phy. Chem. Solids, 29,667, (1968).

72. Kirby, R.D., Hughes, A.F. and Sievers, A.J. : Phy. Rev. B2. 481 (1970).

73. Kaphan, S. & Luty, F. : Solid. State Commn. 6, 907, (1968).

74. Wilson, W.D., Hatcher; R.D., : Phy. Rev. 184. 844 (1969).

Smoluchowski, R. and Dienes, G.J.

75. Mitra, D.N., Agrawal, V.K. & Pandey, G.K. : Solid state Commun. 8, 1645 (1970).
76. Robert, S. : Phy. Rev. 81. 865 (1951).
77. Robert, S. : Ibid. Rev. 76, 1215, (1949).
78. Timme, R.W., Dischler, B. and Estle, T.L. : Phys. Rev. B1. 1610 (1970).
79. Kaphan, S. and Luty, F : Phy. Rev. B15. Aug. (1972).
80. Drey Broadt, W. and Fussgaenger. : Phy. Stat Solids 18, 133 (1966).
81. Alderman, D.W. & Cotts, R.W. : Phy. Rev. B1. 2870 (1970).
82. Wilson, W.D.; Hatcher R.D.; Diences, G.J. & Smoluchowski. : Phy. Rev. 161. 888 (1967).

83. Yang, W. S.; Park, B.-W.; Jung, E. H.; Jeon, N. J.; Kim, Y. C.; Lee, D. U.; Shin, S. S.; Seo, J.; Kim, E. K.; Noh, J. H.; Seok, S. I. Iodide Management in Formamidinium-Lead-Halide−Based Perovskite Layers for Efficient Solar Cells. Science 2017, 356, 1376−1379.
84. Hao, F.; Stoumpos, C. C.; Cao, D. H.; Chang, R. P. H.; Kanatzidis, M. G. Lead-Free Solid-State Organic-Inorganic Halide Perovskite Solar Cells. Nat. Photonics 2014, 8, 489−494.
85. Liang, L.; Gao, P. Lead-Free Hybrid Perovskite Absorbers for Viable Application: Can We Eat the Cake and Have It Too? Adv. Sci. 2018, 5, 1700331.

86. Slavney, A. H.; Leppert, L.; Valdes, A. S.; Bartesaghi, D.Savenije, T. J.; Neaton, J. B.; Karunadasa, H. I. Small-Band-Gap Halide Double Perovskites. Angew. Chem., Int. Ed. 2018, 57, 12765−12770.
87. Zhou, J.; Xia, Z.; Molokeev, M. S.; Zhang, X.; Peng, D.; Liu, Q. Composition Design, Optical Gap and Stability Investigations of Lead-Free Halide Double Perovskite Cs2AgInCl6. J. Mater. Chem. A 2017, 5, 15031−15037.
88. Vargas, B.; Ramos, E.; Pérez-Gutiérrez, E.; Alonso, J. C.; Solis- Ibarra, D. A Direct Bandgap Copper- Antimony Halide Perovskite. J. Am. Chem. Soc. 2017, 139, 9116−9119
89. Kubicki, D. J.; Prochowicz, D.; Hofstetter, A.; Saski, M.; Yadav, P.; Bi, D.; Pellet, N.; Lewiński, J.; Zakeeruddin, S. M.; Grätzel, M.; Emsley, L. Formation of Stable Mixed Guanidinium−Methylammonium Phases with Exceptionally Long Carrier Lifetimes for High- Efficiency Lead Iodide-Based Perovskite Photovoltaics. J. Am. Chem. Soc. 2018, 140, 3345−3351.
90. Filip, M. R.; Hillman, S.; Haghighirad, A. A.; Snaith, H. J. Giustino, F. Band Gaps of the Lead-Free Halide Double Perovskites Cs2BiAgCl6 an Cs2BiAgBr6 from Theory and Experiment. J. Phys Chem. Lett. 2016, 7, 2579−2585.
91. Kojima, A.; Teshima, K.; Shirai, Y.; Miyasaka, T. Organometal Halide Perovskites as Visible-Light Sensitizers for Photovoltaic Cells.J. Am. Chem. Soc. 2009, 131, 6050−6051.
92. Kubicki, D. J.; Prochowicz, D.; Hofstetter, A.; Zakeeruddin, S. M.; Grätzel, M.; Emsley, L. Phase Segregation in Potassium-Doped Lead Halide Perovskites from 39K Solid-State NMR at 21.1 T. J. Am. Chem. Soc. 2018, 140, 7232−7238.
93. Senocrate, A.; Moudrakovski, I.; Kim, G. Y.; Yang, T.-Y. Gregori, G.; Grätzel, M.; Maier, J. The Nature of Ion Conduction in Methylammonium Lead Iodide: A Multimethod Approach. Angew. Chem., Int. Ed. 2017, 56, 7755−7759.

94. Ivanov, Y. N.; Sukhovskii, A. A.; Lisin, V. V.; Aleksandrova, I. P. Phase Transitions of Cs3Sb2I9, Cs3Bi2I9, and Cs3Bi2Br9 Crystals. Inorg. Mater. 2001, 37, 623−627.

ABOUT THE AUTHOR

Dr Mahesh Chandra Mishra is an Associate Professor in the Dept. of Physics at Millat College, Darbhanga, a constituent unit of L.N. Mithila University, Darbhanga , Bihar .

He is gold medalist in M.Sc. and has received his Ph. D. degree in Physics from L.N.M.U. Darbhanga.

RESEARCH ACTIVITIES :

Dr Mishra has published more than a dozen research articles in national and international journals. Also, he has published more than two dozen abstracts in national and international conferences/ seminars proceedings. He has presented more than one dozen papers in national and international seminars and conferences.

He is a life member of research body INDIAN SCIENCE CONGRESS ASSOCIATION (ISCA), KOLKATA. He has completed one UGC sponsored minor research project as a principal investigator. His four research scholars have been awarded Ph.D. degrees.

ABOUT THE BOOK:

In this book, the rotational degrees of freedom of solid molecules is presented with the help of thermal conductivity, specific heat , band-centre and off- centre displacement using CN^- , OH^- and Li^+ ions substituted for the halogens. The book focuses on the shift of the intramolecular vibrational line of OH^- and off-centre direction of impurities in alkali halide crystals as well.

KRIPA DRISHTI PUBLICATIONS

Kripa-Drishti Publications
A-503 Poorva Heights, Pashan-Sus Road, Near Sai Chowk,
Pune – 411021, Maharashtra, India.
Mob: +91 8007068686
Email: editor@kdpublications.in
Web: https://www.kdpublications.in

ISBN: 978-1-716-35980-4